Journal of Medicinal Chemistry

pubs.acs.org/jmc Article

Saturated Hydroxy Fatty Acids Exhibit a Cell Growth Inhibitory Activity and Suppress the Cytokine-Induced β-Cell Apoptosis

Maroula G. Kokotou, Alexandros C. Kokotos,[#] Dimitrios Gkikas,[#] Olga G. Mountanea,[#] Christiana Mantzourani, Abdulaziz Almutairi, Xiaoyong Lei, Sasanka Ramanadham, Panagiotis K. Politis, and George Kokotos*

Cite This: https://dx.doi.org/10.1021/acs.jmedchem.0c00844 Read Online

ACCESS | Metrics & More | Article Recommendations | Supporting Information

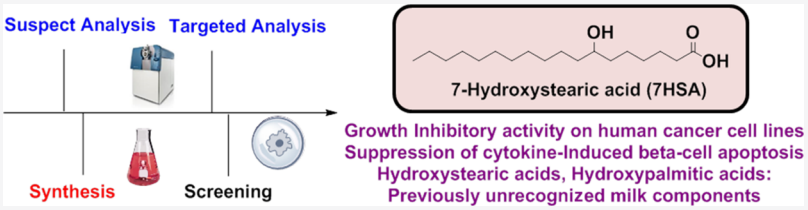

ABSTRACT: The field of bioactive lipids is ever expanding with discoveries of novel lipid molecules that promote human health. Adopting a lipidomic-assisted approach, two new families of previously unrecognized saturated hydroxy fatty acids (SHFAs), namely, hydroxystearic and hydroxypalmitic acids, consisting of isomers with the hydroxyl group at different positions, were identified in milk. Among the various regio-isomers synthesized, those carrying the hydroxyl at the 7- and 9-positions presented growth inhibitory activities against various human cancer cell lines, including A549, Caco-2, and SF268 cells. In addition, 7- and 9-hydroxystearic acids were able to suppress β-cell apoptosis induced by proinflammatory cytokines, increasing the possibility that they can be beneficial in countering autoimmune diseases, such as type 1 diabetes. 7-(*R*)-Hydroxystearic acid exhibited the highest potency both in cell growth inhibition and in suppressing β-cell death. We propose that such naturally occurring SHFAs may play a role in the promotion and protection of human health.

INTRODUCTION

Lipids are increasingly being recognized as biomolecules that dynamically affect human physiology and pathophysiology.[1] Hydroxylated polyunsaturated fatty acids constitute a class of bioactive lipids known for their ability to act as potent signaling mediators. The seminal work of Serhan et al.[2] uncovered a family of protective compounds, termed resolvins (e.g., resolvin E2, **1**, Figure 1a), which promote the resolution of inflammation and are generated from the omega-3 fatty acids docosahexaenoic and eicosapentaenoic. Resolvins together with protectins and maresins constitute a new genus of hydroxylated polyunsaturated fatty acid mediators called specialized proresolving mediators (SPMs).[3,4] In contrast, less is known about the bioactivities of saturated hydroxy fatty acids (SHFAs) and their ability to act as signaling molecules, though some of the SHFAs are relatively common. The 2-hydroxy fatty acids (2HFAs) are abundant in sphingolipids,[5] and the 3-hydroxy fatty acids (3HFAs) are intermediates of fatty acid synthesis and β-oxidation and are constituents of inflammatory lipopolysaccharides.[6] Agonists and antagonists of free fatty acid and hydroxy carboxylic acid receptors have received increased interest in recent years,[7] and medium-chain fatty acids with a hydroxyl group at the 2- or 3-position [e.g., 3-hydroxymyristic acid (3HMA), **2**, Figure 1b] have been shown to activate receptors such as GPR84 more effectively than their nonhydroxylated counterparts.[8,9]

Recently, fatty acid esters of hydroxy fatty acids (FAHFAs), mainly composed of saturated fatty acids, have emerged as a novel class of endogenous lipids with anti-inflammatory and antidiabetic properties.[10] Several branched FAHFAs families have been identified and each family consists of multiple regio-isomers, in which the hydroxyl participating in the ester bond is situated at different positions (5 and higher positions). In particular, the family of palmitic acid (PA) esters of hydroxystearic acids is one of the most abundant and has been recognized as possessing interesting bioactivities.[10,11] For instance, the PA ester of 9-hydroxystearic acid (PAHSA, **3**, Figure 1c) has been reported to activate GPR40, which is important in maintaining glucose homeostasis, and to regulate innate and adaptive immune responses preventing mucosal damage and protecting against colitis.[12−15] Although experi-

Received: June 4, 2020

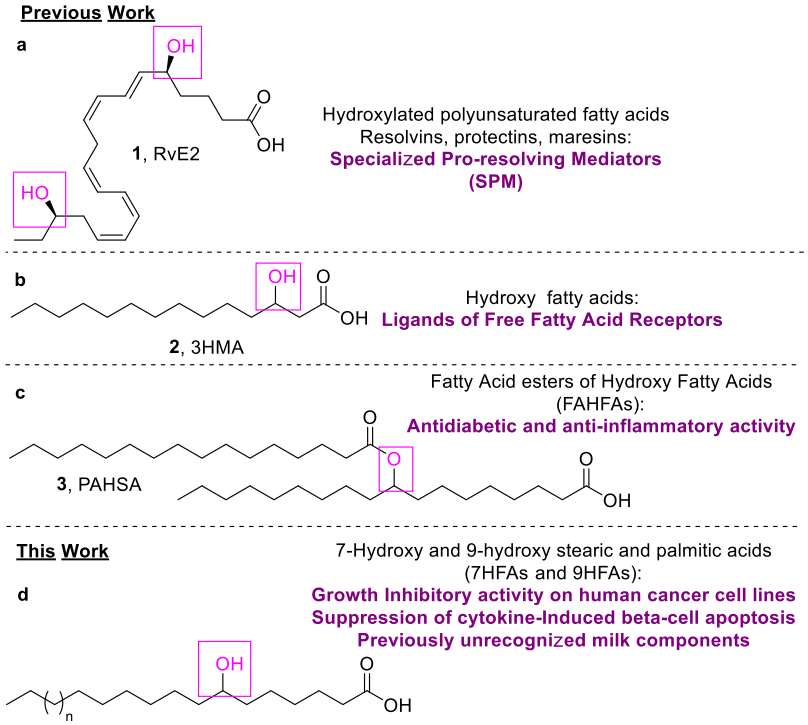

Figure 1. Classes of hydroxylated fatty acids and their bioactivities.

ments in mice have shown that FAHFAs may be generated from SHFAs in vivo,[10] the origin of SHFAs remains unknown. SHFAs bearing a hydroxyl group at a position higher than 3 could be either endogenously generated in the body through a hydroxylation pathway of fatty acids or be obtained exogenously from food.

Lipidomic-based approaches employing mass spectrometry (MS) have been recognized as a powerful and rapidly growing technology that can be used in biomedical research to study disease mechanisms and identify novel therapeutic targets and novel bioactive lipids.[16] Most recently, Watrous et al. utilizing the integration of directed nontargeted MS and computational chemical networking described hundreds of previously unrecognized inflammatory oxylipin metabolites in human plasma, thus providing new insight into the role of oxylipins in human biology.[17]

In view of this, we adopted a lipidomic approach to identify previously unrecognized SHFAs existing in natural sources. Here, we present the asymmetric synthesis of various SHFAs and the study of their bioactivities. We demonstrate that 7-hydroxystearic and 7-hydroxypalmitic acids (7HPA) inhibit cancer cell proliferation and that 7- and 9-hydroxystearic acids exhibit high potency in suppressing cytokine-induced β-cell apoptosis. Further, we report that these effects of SHFAs involve STAT3 signaling pathway, a major player in proproliferative and proinflammatory cascades.

RESULTS

High-Resolution Mass Spectrometry Screening for Masses Corresponding to SHFAs. The presence of 2HFAs and 3HFAs in human plasma[18,19] and foods, in particular in milk,[20,21] is well documented. However, only one report refers to the existence in such sources of two SHFAs possessing the hydroxyl at higher positions (10-hydroxystearic acid and 8-hydroxypalmitic acid).[22] We utilized a "suspect" liquid chromatography (LC)−MS approach with reversed-phase chromatography and high mass accuracy MS operating in full-scan negative mode. In an initial experiment, we screened human plasma and cow milk samples by LC−HRMS and monitored for peaks corresponding to the exact masses (deprotonated molecule) of a set of medium- and long-chain SHFAs, namely, hydroxycaprylic (m/z 159.1027), hydroxycapric (HCA, m/z 187.1340), hydroxy lauric (HLA, m/z 215.1653), hydroxymyristic (HMA, m/z 243.1966), hydroxypalmitic (HPA, m/z 271.2279), hydroxystearic (HSA, m/z 299.2592), hydroxyarachidic (m/z 327.2905), and hydroxybehenic (m/z 355.3218) acids. The accurate mass for each formula was searched using a 0.01 mass width. Among the spectra of the above mentioned medium- and long-chain SHFAs, those of HPAs and HSAs attracted our attention because only weak peaks were recorded for hydroxy caprylic, HCA, HLA, HMA, hydroxy arachidic, and hydroxy behenic acids. Figure 2a,c shows the extracted ion chromatograms (EICs) for reference synthetic 2- and 3-hydroxypalmitic and stearic acids. In a representative human plasma sample, 2HFAs seemed to be the most predominant, with the highest peak intensities corresponding to 2-hydroxypalmitic acid (2HPA) (Figure 2b) and 2HSA (Figure 2d) acids. Corresponding 3HFAs were also evident in the human plasma samples, though they were detected in lower intensities. However, in a representative cow milk sample, although peaks corresponding to 2- and 3-hydroxystearic and PAs (Figure 2f,h) appear at the same retention times with those of reference compounds (relative tolerance of the retention time lower than ±2.5%) (Figure 2e,g), the most intense peaks were recorded at earlier times. These findings suggest the presence of other isobaric regio-isomers (i.e., with the hydroxyl group at positions other than 2- and 3-) in milk.

From the subsequent fragmentation studies, we deduced that the most intense peaks correspond to 7HSA and 10HSA.

https://dx.doi.org/10.1021/acs.jmedchem.0c00844
J. Med. Chem. XXXX, XXX, XXX−XXX

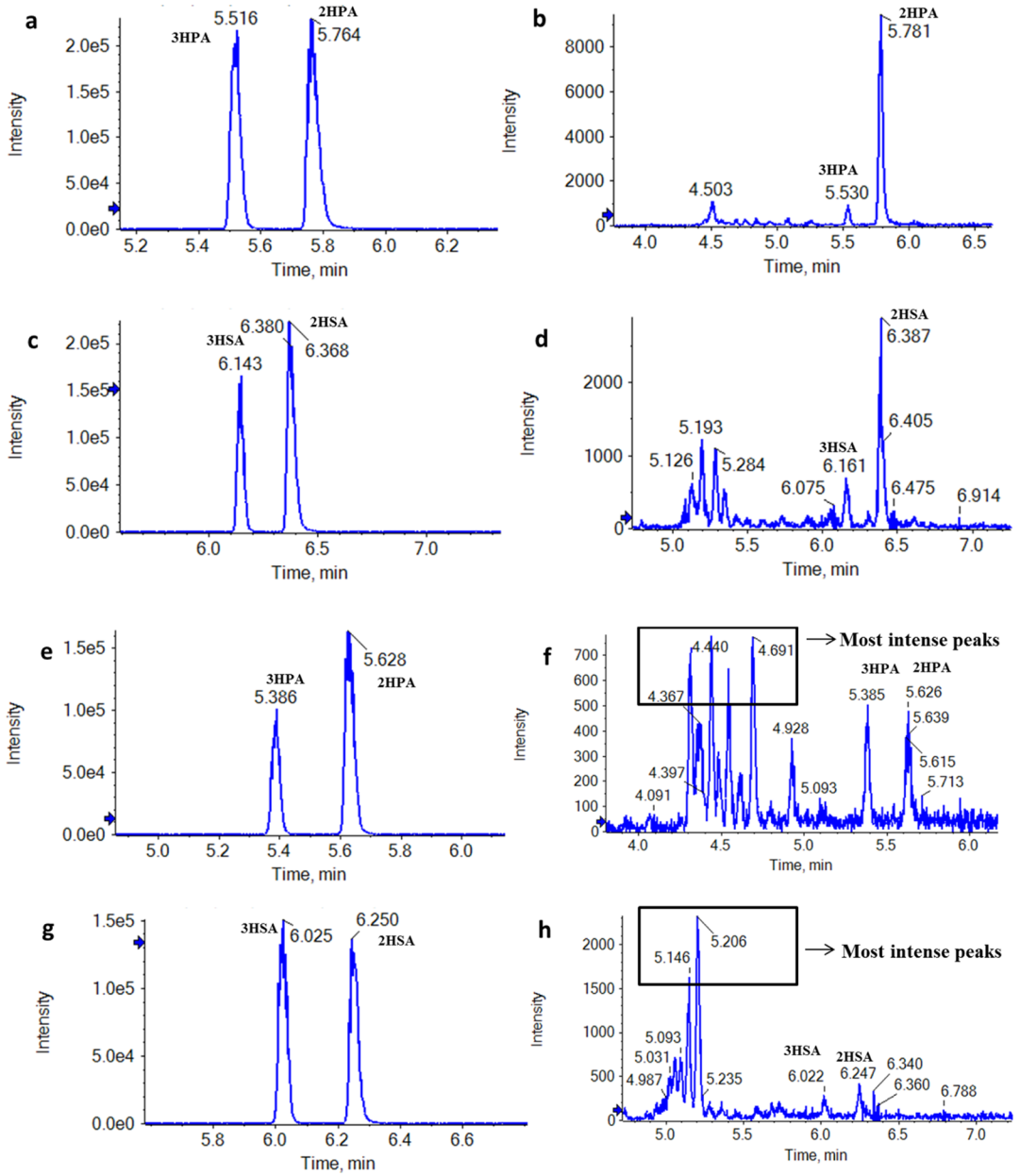

Figure 2. EICs for mass corresponding to hydroxypalmitic acid. (a) Reference compounds; (b) human plasma sample; (e) reference compounds; (f) milk sample. EICs for mass corresponding to hydroxystearic acid. (c) Reference compounds; (d) human plasma sample; (g) reference compounds; (h) milk sample.

To address this further, we proceeded to generate the prerequisite LC−HRMS reference compounds.

Synthesis of 7-Hydroxy and 10-Hydroxystearic and PAs. We have recently reported an enantioselective methodology for the synthesis of FAHFAs and 9-hydroxy fatty acids (stearic and palmitic).[23] In the present study, we followed the same methodology to synthesize saturated 7-hydroxy and 10-hydroxystearic or PAs. The key step consisted of the organocatalytic synthesis of asymmetric terminal epoxides **5a,b** using monoprotected α,ω-diols **4a,b** as starting materials and MacMillan's third-generation imidazolidinone [(2*S*,5*R*)-2-(*tert*-butyl)-3,5-dimethylimidazolidin-4-one trifluoroacetate] as a catalyst for the induction of chirality (Scheme 1). Treatment of epoxides **5a,b** with the appropriate Grignard reagent provided either a 16-atom or an 18-atom carbon chain bearing a hydroxy group at position 7- or 10- (compounds **6a−d**). A sequence of acetylation, hydrogenation, oxidation, and saponification led to (*R*)-HFAs **10a−d** in high enantiomeric purity (Scheme 1). The use of the (2*R*,5*S*)-2-(*tert*-butyl)-3,5-dimethylimidazolidin-4-one trifluoroacetate catalyst enabled the synthesis of the corresponding (*S*)-HFAs.

Determination of Various SHFAs in Milk. To facilitate the identification of the SHFA mixture in milk, we developed a rapid LC−HRMS method that enabled us to simultaneously identify a variety of SHFAs in milk within a 10 min sample run. Six regio-isomers of HPA [2HPA, 3-hydroxypalmitic acid (3HPA), 7HPA, 9-hydroxypalmitic acid (9HPA), 11-hydroxypalmitic acid (11HPA), and 16-hydroxypalmitic acid (16HPA)], six regio-isomers of HSA [2-hydroxystearic acid (2HSA), 3-hydroxystearic acid (3HSA), 7-hydroxystearic acid (7HSA), 9-hydroxystearic acid (9HSA), 10-hydroxystearic acid (10HSA), and 12-hydroxystearic acid (12HSA)], and three

https://dx.doi.org/10.1021/acs.jmedchem.0c00844
J. Med. Chem. XXXX, XXX, XXX−XXX

Scheme 1. Enantioselective Synthesis of SHFAs; (a) PCC, CH_2Cl_2; (b) (i) (2*S*,5*R*)-2-(*tert*-Butyl)-3,5-Dimethylimidazolidin-4-one Trifluoroacetate (20%), 2,3,4,5,6,6-Hexachlorocyclohexa-2,4-dien-1-one, THF; (ii) $NaBH_4$, EtOH; (iii) KOH, EtOH, H_2O; (c) $C_5H_{11}MgBr$ or $C_7H_{15}MgBr$ or $C_8H_{17}MgBr$ or $C_{10}H_{21}MgBr$, CuI, dry THF; (d) AcCl, Pyridine, CH_2Cl_2; (e) H_2, 10% Pd/C, EtOH; (f) Jones Reagent, Acetone; (g) LiOH, THF−H_2O

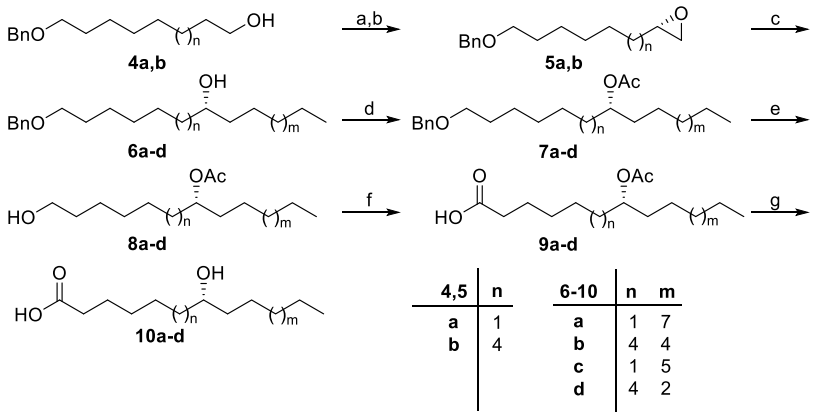

Table 1. Contents of Free SHFAs (ng/mL) in Milk Samples

compound	abbreviation	exact mass $[M-H]^-$	t_r[a]	cow milk (ng/mL), 10 samples, triplicates		
				minimum value	maximum value	mean value ± SD
3-hydroxycapric acid	3HCA	187.1340	3.06	<LOQ[b]	10.1	5.4 ± 1.8[c]
3-hydroxylauric acid	3HLA	215.1653	3.90	<LOQ[b]	36.8	11.9 ± 6.2[c]
16-hydroxypalmitic acid	16HPA	271.2279	4.31	19.3	41.5	26.9 ± 8.2
11-hydroxypalmitic acid	11HPA	271.2279	4.44	20.5	72.6	45.7 ± 18.6
9-hydroxypalmitic acid	9HPA	271.2279	4.56	16.8	45.6	25.5 ± 9.1
7-hydroxypalmitic acid	7HPA	271.2279	4.64	<LOQ[b]	13.1	6.2 ± 4.1[c]
3-hydroxymyristic acid	3HMA	243.1966	4.67	<LOQ[b]	14.9	7.2 ± 3.2[c]
12-hydroxystearic acid	12HSA	299.2592	5.02	<LOQ[b]	21.2	8.5 ± 6.5[c]
10-hydroxystearic acid	10HSA	299.2592	5.11	33.3	218.5	97.5 ± 10.2
7-hydroxystearic acid	7HSA	299.2592	5.17	40.8	378.8	167.3 ± 12.5
9-hydroxystearic acid	9HSA	299.2592	5.32	8.9	42.4	19.5 ± 10.0
3-hydroxypalmitic acid	3HPA	271.2279	5.33	11.0	48.1	28.3 ± 11.2
2-hydroxypalmitic acid	2HPA	271.2279	5.57	10.4	40.8	21.7 ± 9.3
3-hydroxystearic acid	3HSA	299.2592	5.99	10.1	54.4	30.9 ± 18.8
2-hydroxystearic acid	2HSA	299.2592	6.22	10.0	40.9	23.6 ± 12.4

[a]Retention time. [b]Lower of limit of quantification. [c]The mean value was determined using the medium-bound approach.

3HFAs [3-hydroxycapric acid (3HCA), 3-hydroxylauric acid (3HLA), and 3HMA] were used in this study. The analytes and their exact masses lie in the range of 187−300 Da and are summarized in Table 1. As shown in Figure 3a, the 15 reference compounds were distinctly separable with this chromatographic technique. Figure 3b shows a representative chromatogram of a cow milk sample. Ten different cow milk samples were examined in triplicates, and the contents of free HFAs are summarized in Table 1. Details of the analytical method will be published elsewhere.

In an effort to establish the stereochemistry of HPAs and HSAs present in cow milk, the lipid fraction of milk was isolated and a chiral column (Chiralpak AD-RH) was employed for UPLC−HRMS analysis. Using an isocratic elution system consisting of (A) acetonitrile/1% formic acid and (B) water (95/5, v/v) and a long run time (120 min), a nice separation of the peaks corresponding to 3RHPA and 3SHPA was achieved (Figure S3a). In the case of 7HPA and 10HPA, although the peaks corresponding to the enantiomers of 7HPA (7RHPA and 7SHPA) and 10HPA (10RHPA and 10SHPA) are well separated from each other, overlap of the peaks of 7SHPA and 10RHPA was observed (Figure S3a). The EIC of the lipid fraction of a cow milk sample clearly suggests that both enantiomers of 3HPA are present in milk (Figure S3b). The simultaneous presence of various positional isomers and enantiomers of HPAs in a real milk sample complicates the identification of the various enantiomers, preventing any conclusive results under these conditions (Figure S3b). Similar results were obtained for HSAs (data not shown).

Cell Growth Inhibitory Effects of SHFAs on Human Cancer Cell Lines. In 1991, HSA was identified as a peroxidation product in Lewis lung carcinoma cells.[24] Subsequently, it was reported that 9HSA upregulates p21WAF1 in HT29 cancer cells,[25] inhibits cell growth in human colon cancer targeting histone deacetylase 1,[26] interferes with EGF signaling in a human colon adenocarcinoma,[27] and modulates apoptotic signaling in osteosarcoma cells.[28] We, therefore, sought to determine the effects of our recently identified milk SHFAs on proliferation of human cancer cell lines: epithelial lung carcinoma (A549), colorectal adenocarcinoma (Caco-2), brain glioblastoma (U87-MG), and astrocytoma (SF268). The MTT assay was utilized to assess viable cell numbers.[29]

https://dx.doi.org/10.1021/acs.jmedchem.0c00844
J. Med. Chem. XXXX, XXX, XXX−XXX

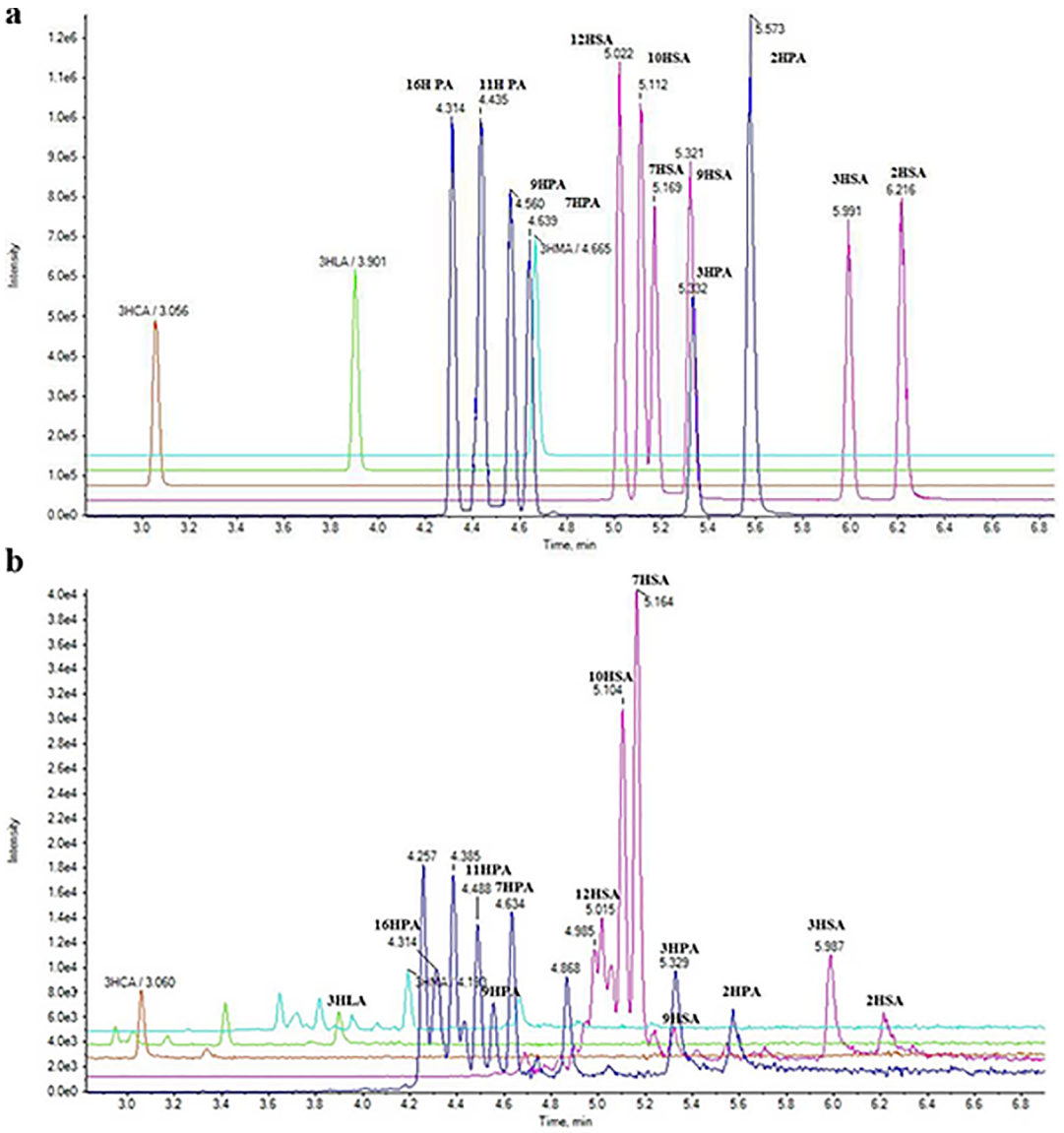

Figure 3. EICs of SHFAs. (a) Standard solution (500 ng/mL). (b) Representative cow milk sample.

The growth inhibitory effects of eight enantiomers of HSAs and five enantiomers of HPAs (10, 25, 50, and 100 μM) on A549, Caco-2, and SF268 cells are summarized in Figure 4a,c,e, respectively. Interestingly, the position of the hydroxyl functionality in the long-chain drastically influences the in vitro potency. In general, 7HSA and 9HSA, as well as the corresponding PAs, exhibited statistically significant inhibitory potency at concentrations over 25 μM, while when the hydroxyl group is at position 2-, 10-, or 12- of the stearic chain or at position 10- of the palmitic chain, only very weak activity was observed. All statistical comparisons for inhibitory potency of the investigated HFAs are included in Table 1S. The IC_{50} values for the enantiomers 7RHPA, 7SHPA, 7RHSA, and 7SHSA were calculated from the curves depicted in Figure 4b,d,f, respectively, and vary within the range of 27−55 μM. 7-(*R*)-Hydroxystearic acid (7RHSA) was found to exhibit the highest growth inhibitory potency (IC_{50} values 38, 37, and 27 μM for A549, Caco-2, and SF268 cells, respectively), being clearly more potent than its regio-isomer, 9RHSA. The (*R*)-enantiomer of 7HSA was found to be slightly more potent than the (*S*)-enantiomer (IC_{50} 38 vs 50 μM in A549, 37 vs 50 μM in Caco-2, and 27 vs 47 μM in SF268 cells). In the case of 7HPA, the (*R*)-enantiomer was found to be almost equipotent with the (*S*)-enantiomer (IC_{50} 49 vs 55 μM in A549 and 42 vs 50 μM in Caco-2 cells). The growth inhibitory effect of various HSAs and HPAs on U87-MG cell line is depicted in the Supporting Information (Figure S1). None of SHFAs tested presented inhibitory activity on U87-MG, indicating a cell-specific activity.

The growth inhibitory effect of PA and stearic acid (SA) was studied in A549, Caco-2, and SF286 cells for comparison purposes, and the results are shown in Figure 4a,c,e. A very weak effect was observed only for stearic acid, proving that the presence of the hydroxyl group at a particular position determines the cell growth inhibitory potency. In addition, the growth inhibitory effect of 7PAHSA was studied in A549, Caco-2, and SF286 cells. No effect was observed at concentrations up to 100 μM (Figure 4a,c,e). Similar negative results were observed for 9PAHSA and 9OAHSA (Figure 4a,c,e). These findings exclude the possibility that the growth inhibitory effect is caused by FAHFAs that may be generated in cells after treatment with HSA.

https://dx.doi.org/10.1021/acs.jmedchem.0c00844
J. Med. Chem. XXXX, XXX, XXX−XXX

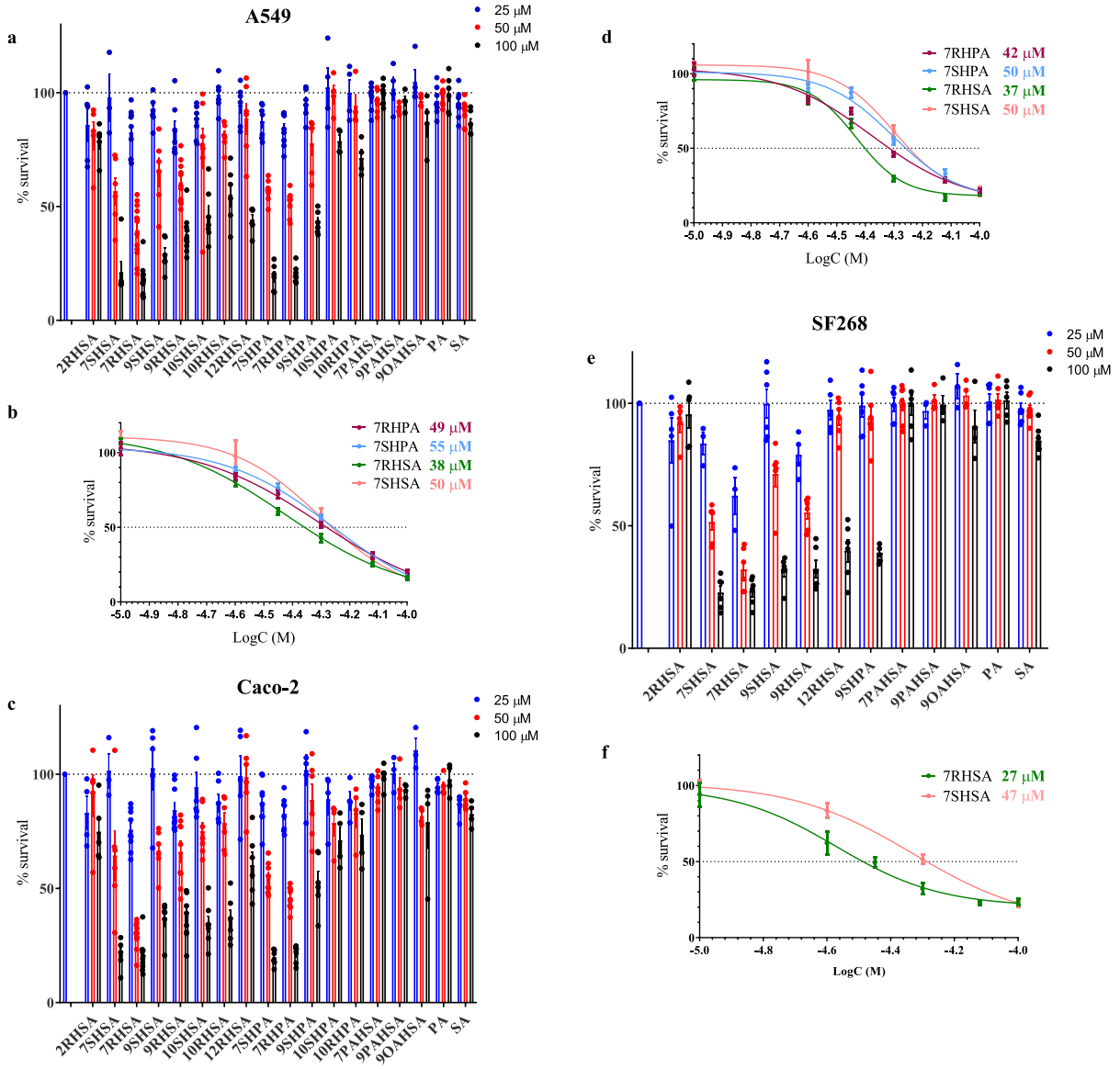

Figure 4. Cell growth inhibitory potency of various HSAs and HPAs. (a) Human cancer cell line A549. (c) Human cancer cell line Caco-2. (e) Human cancer cell line SF268. Cells were treated with increasing concentrations (10, 25, 50, and 100 μM) of the test compounds for 72 h, and cell viability was determined by the MTT assay for a minimum of six experiments (AVG ± SEM). No effect was observed for any compound at 10 μM and this concentration is not shown in the graph. (b) IC_{50} values (μM) of enantiomers 7RHPA, 7SHPA, 7RHSA, and 7SHSA in A549 cells. IC_{50} values were derived from the dose−response relationship for a minimum of six experiments (95% CI log IC_{50} −4.49 to −4.36, −4.42 to −4.20, −4.38 to −4.14, and −4.43 to −4.17, respectively). (d) IC_{50} values (μM) of enantiomers 7RHPA, 7SHPA, 7RHSA, and 7SHSA in Caco-2 cells. IC_{50} values were derived from the dose−response relationship for a minimum of six experiments (95% CI log IC_{50} −4.46 to −4.40, −4.43 to −4.32, −4.36 to −4.25, and −4.36 to −4.24, respectively). (f) IC_{50} values (μM) of enantiomers 7RHSA and 7SHSA in SF268 cells. IC_{50} values were derived from the dose−response relationship for a minimum of six experiments (95% CI log IC_{50} −4.71 to −4.43, −4.47 to −4.19, respectively).

To understand the mode of action of SHFAs, A549 cells were incubated with 7RHSA, which exhibited the highest potency, or its regio-isomer 9RHSA (50 μM) for 72 h and then fixed for immunostaining and cell imaging. Markers of cell cycle [phosphorylated histone H3 (pH3)[30] and apoptosis [activated caspase 3 (casp3)[31] were used to investigate their antiproliferative mechanism. These analyses revealed that both 7RHSA and 9RHSA induced the arrest of the cell cycle (Figure 5a), as reflected by the decreased phosphorylation of the histone H3 marker (pH3), but did not promote apoptosis (Figure 5b), as evidenced by the absence of increased generation of activated caspase-3.

Subsequently, mRNA analysis was employed to assess which signaling pathway(s) leading to the cell cycle arrest is affected by 7RHSA. A variety of different signaling molecules, namely, cyclin D1, cyclin E1, $p21^{cip1}$, $p27^{kip1}$, EGFR, PI3K (PIK3CA), p53, mTOR, cmyc, RET, and STAT3 (Figure 6a−k), were examined by real-time RT-qPCR. This approach revealed a specific reduction of the transcription regulator signal transducer and activator of transcription 3 (STAT3) mRNA (Figure 6k). Most importantly, the downregulation of STAT3 expression was observed both at mRNA and protein levels of both total and phosphorylated STAT3 (p-STAT3) (Figure 6l−n). The latter event is critical for STAT3-mediated proproliferative and proinflammatory effects, indicating a

https://dx.doi.org/10.1021/acs.jmedchem.0c00844
J. Med. Chem. XXXX, XXX, XXX−XXX

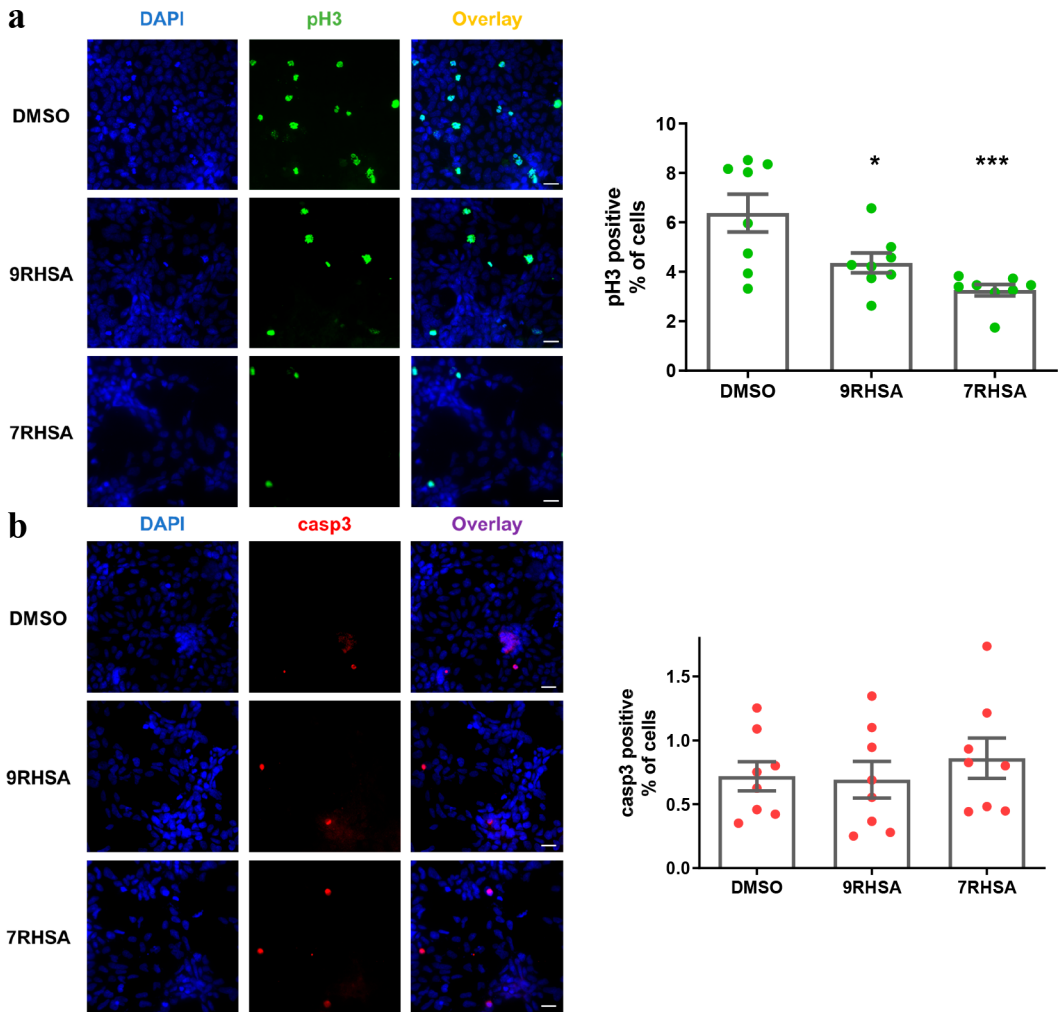

Figure 5. Effect of 7RHSA and 9RSHA on cell death and apoptosis of A549 cells. Cells were treated with 50 μM 7RHSA, 9RSHA, and equivalent vehicle (DMSO) for 72 h and then immunostained against (a) phosphorylated histone H3 (pH3) and (b) activated caspase 3 (casp3) to further study their action. Representative images are shown as well as quantification of the percentage of positive-stained cells, as identified by DAPI staining (n = 8 fields of view, AVG ± SEM).

possible involvement of 7RHSA compound in suppressing these functions.

Suppression of Cytokine-Induced β-Cell Apoptosis by Hydroxystearic Acids. As discussed in Introduction, FAHFAs have been shown to exhibit attractive antidiabetic properties.[10−12] Recently, it has been reported that PAHSAs promote β-cell survival and function and protect against type 1 diabetes (T1D).[32] However, nothing is known about such an activity of SHFAs. To examine the potential impact of SHFAs on β-cell survival, INS-1 cells were treated with proinflammatory cytokines (CTKs) (IL-1β and IFNγ) in the absence or presence of four different enantiomers of 7- and 9-hydroxystearic acids (1 or 10 μM), namely, 7RHSA, 7SHSA, 9RHSA, and 9SHSA, and the results are shown in Figure 7. None of them alone had a significant effect on cell survival, in comparison with vehicle alone. As expected, CTK alone promoted cell death (15−23%) relative to vehicle alone. At 1 μM, 9RHSA and 9SHSA, but not 7RHSA and 7SHSA, reduced cell death (ca. 40%), relative to CTK alone. At 10 μM, cell death was further significantly decreased by 9RHSA (73%), 7RHSA (95%), and 9SHSA (68%); however, 7SHSA did not promote a significant decrease, relative to CTK alone. These findings suggest differential effects of the four HSAs in protecting β-cells against cytokine attack.

The inhibitory effect of 7PAHSA, which might be generated in cells after the treatment with 7HSA, was studied in INS-1 cells at a concentration of 10 μM. As shown in Figure 7e, a weak effect was observed, leading to the conclusion that the potent effect observed for 7HSA at a concentration of 10 μM should be mainly attributed to 7RHSA by itself.

It is well-established that saturated and monounsaturated FFAs cause apoptosis of β-cells. Numerous studies performed with insulinoma cell lines, human β-cell lines, murine, and human islets demonstrate profound β-cell apoptosis following exposure to either palmitate or stearate,[33−38] analogous to proinflammatory cytokine-induced β-cell apoptosis.

DISCUSSION

Initially, a "suspect" LC−HRMS analysis of human plasma and cow milk samples revealed the presence of novel SHFAs, bearing the hydroxyl group at positions other than 2- and 3-, in milk but not plasma. A variety of SHFAs were synthesized and a rapid LC−HRMS method for the simultaneous determination of 15 synthetic SHFAs was developed. Six regio-isomers of HPA, six regio-isomers of HSA, and three additional 3HFAs

https://dx.doi.org/10.1021/acs.jmedchem.0c00844
J. Med. Chem. XXXX, XXX, XXX−XXX

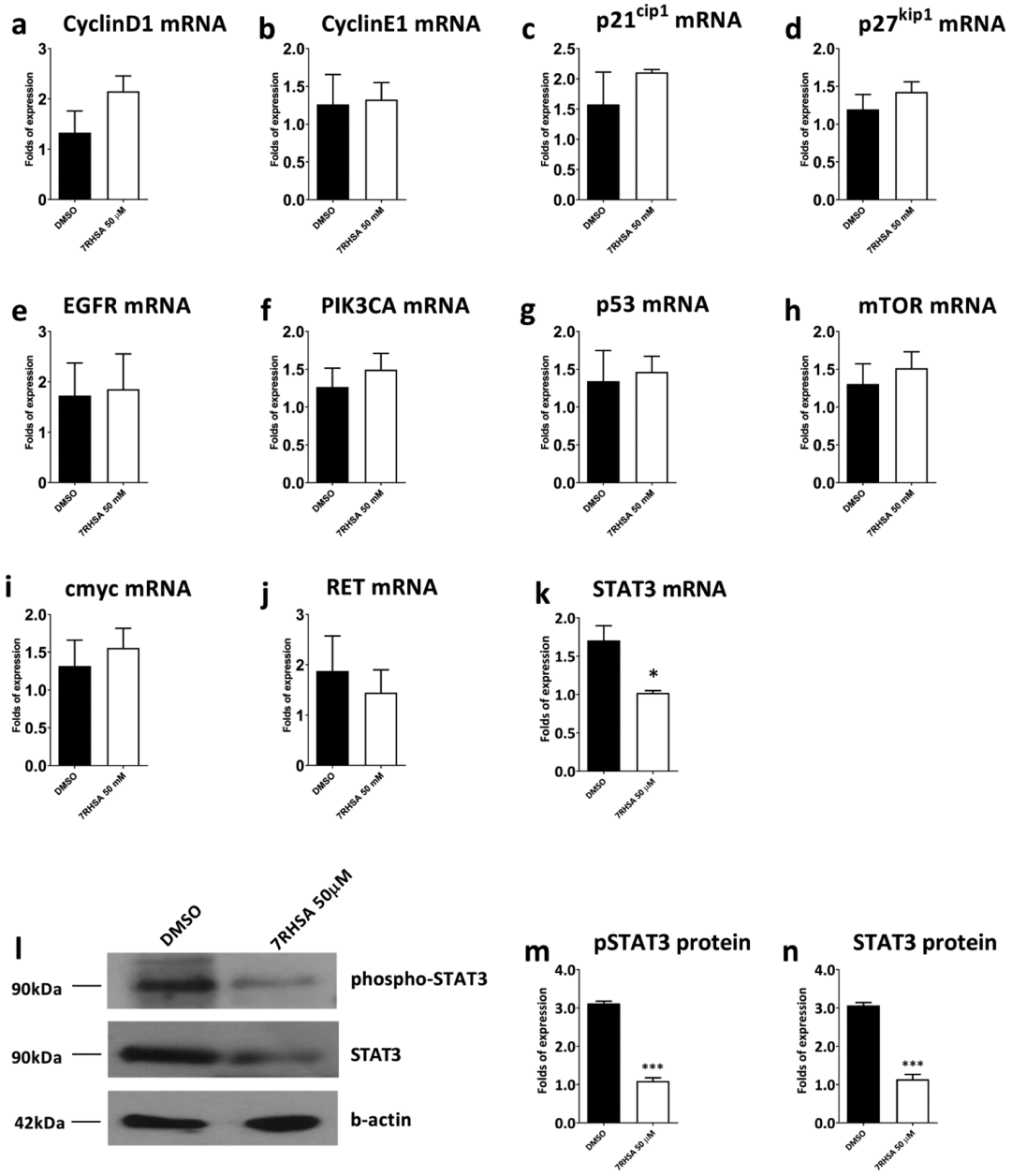

Figure 6. Effect of 7RHSA on crucial cell growth and proliferation regulators. (a–j) Relative expression levels of cyclinD1, cyclinE1, $p21^{cip1}$, $p27^{kip1}$, EGFR, PIK3CA (PI3K), p53, mTOR, cmyc, and RET mRNA in DMSO- and 7RHSA-treated A549 cells, measured with quantitative real-time RT-PCR. (k) Relative expression levels of STAT3 mRNA in DMSO- and 7RHSA-treated A549 cells, measured with quantitative real-time RT-PCR. (l) Western blots for phospho-STAT3, STAT3, and b-actin protein in DMSO- and 7RHSA-treated A549 cells. (m,n) Relative expression of phospho-STAT3 and STAT3 proteins in DMSO- and 7RHSA-treated A549 cells.

were well separated by this method, and their concentrations in samples of cow milk were quantifiable. Our LC–HRMS study uncovered the presence of previously unrecognized families of naturally occurring SHFAs in milk. Each family consists of regio-isomers of a particular fatty acid (e.g., stearic acid) hydroxylated at various positions (e.g., 7, 9, 10, etc.). In cow milk, 7HSA and 10HSA are the predominant HFAs with an 18-carbon saturated chain, and they were present in considerably higher concentrations (167.3 ± 12.5 and 97.5 ± 10.2 ng/mL, respectively) than other detected SHFAs. In the seminal work of Kahn et al.,[10] it was demonstrated that gavage of mice with 9-hydroxyheptadecanoic acid resulted in the synthesis of FAHFAs containing this fatty acid, indicating that FAHFAs can be synthesized in vivo. Thus, SHFAs (e.g., 7-, 9-, 10-) present in foods and taken by humans in daily dietary intake may serve as the precursors of the physiologically relevant corresponding FAHFAs, although the direct hydroxylation (enzymatic or nonenzymatic) of SHFAs within the body cannot be excluded.

The in vitro growth inhibition study using the MTT viability assay demonstrated that the (*R*)-enantiomer of 7HSA exhibited the highest potency (IC_{50} values of 38, 37, and 27 μM against human cancer cells A549, Caco-2, and SF268, respectively) among the HFAs tested, being more potent than the corresponding 9HSA and the other regio-isomers (2-, 10-, 12-). The (*R*)-enantiomer of 7HSA exhibited slightly higher potency than the (*S*)-enantiomer (IC_{50} 38 vs 50 μM in A549 and 37 vs 50 μM in Caco-2 cells). In the case of HPAs, again

https://dx.doi.org/10.1021/acs.jmedchem.0c00844
J. Med. Chem. XXXX, XXX, XXX–XXX

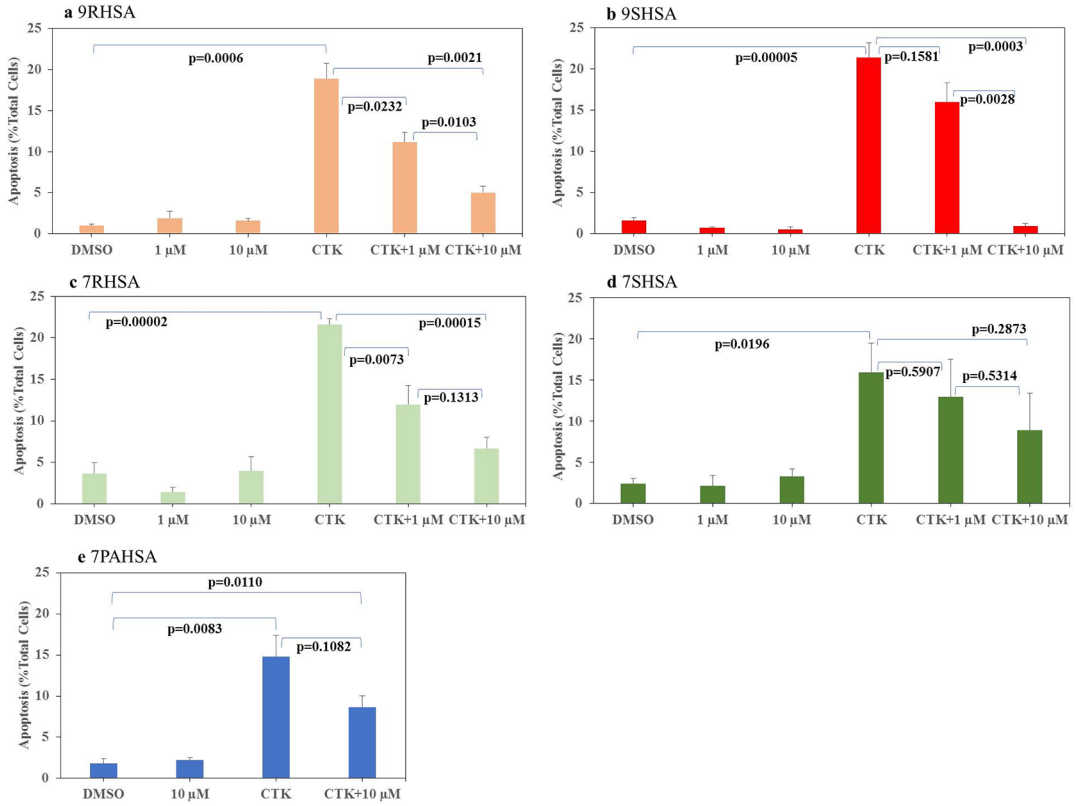

Figure 7. Comparison of the effects of SHFA enantiomers on β-cell apoptosis. INS-1 insulinoma cells were cultured in six-well plates to 70% confluency at 37 °C under an atmosphere of 5% CO_2/95% air. The cells were then pretreated with vehicle (DMSO) or the enantiomers (1 or 10 μM) for 1 h. The cells were then exposed to vehicle alone or CTK (20 ng/mL IL-1β + 200 ng/mL IFNγ) for 16 h. (a) 9RHSA; (b) 9SHSA; (c) 7RHSA; (d) 7SHSA; (e) 7PAHSA. The cells were then processed for TUNEL analyses to determine the extent of apoptotic cell death. The data are the mean ± SEM of apoptotic cells, relative to total cell number, and were generated from three to five independent experiments.

7HPA exhibited higher potency than 9HPA and 10HPA, while the (*R*)-enantiomer was found almost equipotent with the (*S*)-enantiomer. The observation that none of SHFAs exhibited growth inhibition on U87-MG cells indicated a cell-specific effect. PA and SA did not cause any effect in A549, Caco-2, and SF268 cells, highlighting the importance of a hydroxyl functionality at a particular distance from the carboxyl group of the fatty chain. No effect was also caused by 7PAHSA, 9PAHSA, and 9OAHSA, indicating that acylation of the hydroxyl functionality by a fatty chain destroys the growth inhibitory potency.

The mechanism CORRECT of cell proliferation inhibition was attributed to the ability to arrest the cell cycle while not interfering with cell apoptosis. This phenotype was further attributed to reduction in STAT3, a transcription factor that regulates the expression of genes related to cell cycle, cell survival, and immune response.[39] STAT3 is activated by CTK and growth factors through kinase-mediated tyrosine phosphorylation and dimerization,[40] leading to a nuclear translocation and transcription activation. Recently, it has been demonstrated that STAT3 is post-translationally S-palmitoylated at the SRC homology 2 domain, which also promotes its dimerization and transcriptional activation.[41] Although in normal cells, activation of STAT3 signaling is transient and controlled, STAT3 remains constitutively active in approximately 70% of human solid and hematological tumors.[42] Prolonged STAT3 activation has been heavily implicated in tumorigenesis, while increased STAT3 levels correlate with poor patient prognosis,[42] and as a consequence, the STAT3 signaling pathway represents an attractive drug target for cancer therapy. Although a variety of small-molecule STAT3 inhibitors have been developed,[43,44] the traditional orthosteric inhibitors of STAT3 have shown to exhibit limited clinical efficacy, with low selectivity and numerous side effects. Therefore, allosteric inhibitors targeting STAT3 or its upstream molecules have emerged as a more promising approach.[44] The STAT3 mRNA reduction uncovered here provides a very promising mechanism for cell cycle arrest and suggests that the post-translation modification levels of STAT3 can also be affected. Overall, our cell biology analyses render this new class of naturally existing substances as promising novel antiproliferative and anti-inflammatory agents.

Pancreatic β-cells are central players in the pathogenesis of both T1D and T2D and a decrease in β-cell number and/or deficiency in the function of existing β-cells contribute to the development of the disease. Therefore, there is an increasing effort to identify novel methods of improving the number and function of β-cells.[45] Dysregulated cytokine signaling resulting to β-cell apoptosis has been targeted by either genetic or small-molecule approaches.[45] Along this line, we have previously identified small-molecule inhibitors of calcium-independent phospholipase A_2 able to suppress the cytokine-induced β-cell apoptosis.[46,47] In view of their effects in cancer cells described above, we sought to assess the effects of SHFAs on β-cell apoptosis. INS-1 insulinoma cells were treated with proinflammatory CTK, recognized as mediators of β-cell death leading to T1D. As expected, CTK exposure promoted ca. 20–25% apoptotic cell death. Cotreatment with four HSAs

https://dx.doi.org/10.1021/acs.jmedchem.0c00844
J. Med. Chem. XXXX, XXX, XXX−XXX

produced differential effects: the 9HSAs, but not the 7HSAs, significantly inhibited apoptosis at 1 μM. At 10 μM, both of the (*R*)-enantiomers promoted further inhibition of apoptosis, with the 7RHSA nearly completely inhibiting apoptosis. In contrast, 9SHSA did not promote such a marked decrease in cell death, while 7SHSA exhibited the weakest effects. These finding suggest that the (*R*)-enantiomer of 7HSA is a more potent inhibitor of β-cell death than the (*S*)-enantiomer. Importantly, these HFAs warrant consideration as small-molecule inhibitors that may be effective in preventing autoimmune destruction of β-cells and counter development of T1D. The ability of 7HSA to suppress the apoptosis of β-cells is in direct contrast to the effect reported for PA and SA,[33−38] which cause apoptosis of β-cells.

Kahn et al. have recently reported that PAHSAs promote β-cell survival and function and protect against T1D.[32] In the present study, we demonstrate that simple, not esterified, HSAs (either 7- or 9-) are able to protect β-cells from cytokine-induced apoptosis. It seems that only the hydroxy fatty acid part of PAHSAs is enough to produce the beneficial effect in β-cells. If we consider potential exogenous administration as a therapeutic strategy for β-cell protection, it is advantageous and more attractive to use HFAs instead of FAHFAs because HFAs may be synthesized more easily in comparison to the more complex structured FAHFAs, avoiding additional steps for synthesizing the esterified FAHFAs from HFAs. Furthermore, as recently demonstrated in mice, FAHFAs may be metabolized in vivo by the endogenous hydrolases AIG1 and ADTRP.[48]

The potential health benefits from the consumption of milk fatty acids have been recently reviewed discussing that whole dairy products could promote human health because of the presence of certain bioactive fatty acids.[49] There is considerable evidence, although not conclusive, that an increased consumption of milk or dairy products is associated with a reduction in colon cancer.[50−52] However, the role of milk fat content in cancer prevention remains unclear. In the present study, we demonstrate that milk contains previously unrecognized lipid components, such as 7-hydroxy and 9-hydroxy stearic acids and PAs, which inhibit in vitro growth of human cancer cell lines, including the epithelial colorectal adenocarcinoma line Caco-2, with IC_{50} values between 40 and 75 μM. It has to be noted that a number of SHFAs are present in milk, contributing to a cumulative effect. Thus, the newly uncovered naturally occurring milk components SHFAs may constitute a novel class of chemopreventive agents analogous to the plant food components flavonoids, which are polyphenols with a recognized protective role in tumor development. A detailed comparative analysis has shown that flavonoids possess growth inhibitory effects in different cancer cell lines with IC_{50} values ranging from 40 to 200 μM.[53] The results of the present study could suggest that SHFAs might play a cancer preventive role, especially in the intestinal tract because of direct exposure of intestinal epithelia to these dietary milk ingredients.

The association between milk fatty acids intake and T2D is not well established.[54] Saturated fatty acids such as PA could increase the risk of T2D. However, milk also contains several other fatty acids that are beneficial for human health. A recent large meta-analysis, which pooled the findings from 16 prospective cohort studies, discusses the potential health effects of selected dairy products, highlighting that higher levels of odd-chain saturated fatty acids C15:0 and C17:0 are associated with a lower risk of T2D.[55] Another study in the Dutch population has shown that total SFAs do not relate to T2D risk, but the association may depend on the type and food sources of the SFAs. For example, individual SFAs that are commonly found in cheese were significantly related to lower T2D risks.[56] The previously unrecognized SHFAs described in the present study may contribute to lower the risk of T2D by milk consumption.

CONCLUSIONS

In summary, we identified two previously unrecognized families of fatty acids in milk consisting of regio-isomers possessing the hydroxyl functional group at different positions and we demonstrated that the 7- and 9-hydroxystearic and PAs manifest cell growth inhibitory properties as well as suppression of cytokine-induced β-cell apoptosis. 7-(*R*)-Hydroxystearic acid exhibited the highest potency both in cell growth inhibition and in suppressing the β-cell death in INS-1 cells. The research workflow we followed in the present work, that is, "suspect" LC−HRMS analysis in a food matrix—organic synthesis—targeted LC−HRMS analysis using reference compounds in this food matrix—study of the in vitro bioactivities, may be employed in searching other food matrices, providing a foundation for the discovery of previously unrecognized naturally occurring lipids that may play a role in the protection and promotion of human health.

EXPERIMENTAL SECTION

General. All commercially available products and solvents were purchased from Sigma-Aldrich, Fluka, Merck, and Alfa Aesar. Solvents were used as received or dried over molecular sieves (4 Å). All water- or air-sensitive reactions have been performed under an argon atmosphere with dry solvents and anhydrous conditions. All reactions were monitored by thin-layer chromatography performed on aluminum-backed silica plates (0.2 mm, 60 F254). Purification by flash chromatography was performed on Merck silica gel 60 (230−400 mesh). Melting points were determined using a Buchi 530 apparatus and were uncorrected. Optical rotations were measured using a PerkinElmer 343 polarimeter in a 10 cm cell at room temperature. ^{1}H and ^{13}C NMR spectra were recorded on a Varian Mercury (200 and 50 MHz, respectively) or a Bruker AVANCE NEO (400 and 100 MHz, respectively) in $CDCl_3$. Chemical shifts δ are given in parts per million, and coupling constants (J) are given in Hz. Peak multiplicities are described as follows: s, singlet, d, doublet, t, triplet, and m, multiplet. High-resolution mass spectra were obtained on a Bruker Maxis Impact QTOF spectrometer or an AB Sciex 4600 Triple TOF mass spectrometer. The purity of all compounds subjected to biological tests was determined by analytical high-performance liquid chromatography (HPLC) and was found to be ≥95%. For the measurement of enantiomeric excess (ee) of **5a,b**, HPLC experiments were performed on an Agilent 1100 Series with a DAD UV detector, and the peak intensities were measured in the UV range between 206 and 280 nm. A Daicel Chiralpak OD-H chromatography column (250 × 4.6 mm ID) was used with HPLC grade hexane and ^{i}PrOH as solvents.

2HPA, 2HSA, and 16HPA were commercially available. 3HCA, 3HLA, 3HMA, 3HPA, and 3HSA were synthesized as previously described, and their analytical data are in accordance with the literature.[57] 9HPA, 9HSA, 11HPA, and 12HSA were synthesized as previously described, and their analytical data are in accordance with the literature.[23]

General Procedure for the Synthesis of Epoxides (*S*)-5a,b and (*R*)-5a,b. To a solution of (2*S*,5*R*)-2-(*tert*-butyl)-3,5-dimethylimidazolidin-4-one trifluoroacetate (for *S*-epoxide) or (2*R*,5*S*)-2-(*tert*-butyl)-3,5-dimethylimidazolidin-4-one trifluoroacetate (for *R*-epoxide) (57 mg, 0.20 mmol) in THF (0.5 mL), 2,3,4,5,6,6-

https://dx.doi.org/10.1021/acs.jmedchem.0c00844
J. Med. Chem. XXXX, XXX, XXX−XXX

hexachlorocyclohexa-2,4-dien-1-one (381 mg, 1.10 mmol) was added, followed, after 5 min, by the corresponding aldehyde (1.00 mmol). After stirring for 20 min at room temperature, the resulting mixture was cooled to 0 °C before $NaBH_4$ (95 mg, 2.50 mmol) and EtOH (1 mL) were added. After 10 min, the mixture was warmed to room temperature for 5 min before a freshly prepared solution of aqueous KOH (1.70 g KOH diluted in 2.7 mL of water) and EtOH (1.3 mL) were added. The resulting mixture was stirred vigorously for 30 min, and then, water (20 mL) was added. The mixture was extracted with Et_2O (3 × 20 mL), washed with brine (1 × 20 mL), dried over Na_2SO_4, filtered, and concentrated under reduced pressure. The epoxide was purified by silica gel flash chromatography eluting with petroleum ether (bp 40−60 °C)/ethyl acetate 8/2 or 7/3.

*(S)-2-(6-(Benzyloxy)hexyl)oxirane (S)-**5a**.* Colorless oil; yield 68%; ^{1}H NMR (200 MHz, $CDCl_3$): δ 7.45−7.14 (5H, m, ArH), 4.50 (2H, s, $ArCH_2$), 3.46 (2H, t, *J* = 6.5 Hz, OCH_2), 2.89−2.80 (1H, m, OCH), 2.73 (1H, t, *J* = 4.5 Hz, OCH), 2.45 (1H, dd, *J* = 5.0, 2.7 Hz, OCH), 1.65−1.22 (10H, m, 10 × C*H*H); ^{13}C NMR (50 MHz, $CDCl_3$): δ 138.5, 128.3, 127.5, 127.4, 72.8, 70.3, 52.3, 47.0, 32.3, 29.6, 29.2, 26.0, 25.9; $[\alpha]_D^{20}$ −5.0 (*c* 1.0, CH_2Cl_2); HRMS (ESI^+) *m*/*z*: calcd for $C_{15}H_{22}O_2Na^+$, 257.1512; $[M + Na]^+$ found, 257.1512; HPLC analysis: 93% ee.

*(R)-2-(6-(Benzyloxy)hexyl)oxirane (R)-**5a**.* Colorless oil; yield 78%; $[\alpha]_D^{20}$ +6.0 (*c* 1.0, CH_2Cl_2); lit.[58] for (*R*)-epoxide $[\alpha]_D^{25}$ +5.6 (*c* 2.0, $CHCl_3$).

*(S)-2-(9-(Benzyloxy)nonyl)oxirane (S)-**5b**.* Colorless oil; yield 75%; ^{1}H NMR (200 MHz, $CDCl_3$): δ 7.44−7.16 (5H, m, ArH), 4.50 (2H, s, $ArCH_2$), 3.46 (2H, t, *J* = 6.6 Hz, OCH_2), 2.97−2.84 (1H, m, OCH), 2.74 (1H, t, *J* = 4.5 Hz, OCH), 2.46 (1H, dd, *J* = 5.0, 2.8 Hz, OCH), 1.73−1.15 (16H, m, 16 × C*H*H); ^{13}C NMR (50 MHz, $CDCl_3$): δ 138.7, 128.3, 127.6, 127.4, 72.8, 70.5, 52.4, 47.1, 32.5, 29.7, 29.5, 29.4, 26.1, 25.9; $[\alpha]_D^{20}$ −4.0 (*c* 1.0, CH_2Cl_2); lit.[59] for (*S*)-epoxide $[\alpha]_D^{20}$ −4.2 (*c* 1.0, $CHCl_3$); HRMS (ESI^+) *m*/*z*: calcd for $C_{18}H_{28}O_2Na^+$, 299.1982; $[M + Na]^+$ found, 299.1977; HPLC analysis: 92% ee.

*(R)-2-(9-(Benzyloxy)nonyl)oxirane (R)-**5b**.* Colorless oil; yield 75%; $[\alpha]_D^{20}$ +3.6 (*c* 1.0, CH_2Cl_2); lit.[59] for (*R*)-epoxide $[\alpha]_D^{23}$ +3.9 (*c* 1.0, $CHCl_3$).

General Procedure for the Synthesis of Compounds (*R*)-6a−d and (*S*)-6a−d. To a flame-dried flask which contained copper(I) iodide (40 mg, 0.20 mmol) under an inert atmosphere, pentylmagnesium bromide (or heptylmagnesium bromide or octylmagnesium bromide or decylmagnesium bromide) (2 M solution in diethyl ether, 2 mL, 2.00 mmol) was added. After cooling to −40 °C and stirring for 10 min, epoxide **5a,b** (1.00 mmol) in dry THF (10 mL) was added dropwise. The mixture was left stirring at −40 °C for 1 h and then warmed to room temperature. Then, a saturated aqueous solution of NH_4Cl (10 mL) was added, and the aqueous layer was extracted with Et_2O (3 × 20 mL). The organic phase was washed with brine (1 × 50 mL), dried over Na_2SO_4, filtered, and concentrated under reduced pressure. The alcohol was obtained by flash silica chromatography eluting with petroleum ether (bp 40−60 °C)/ethyl acetate 8/2 or 7/3.

*(R)-1-(Benzyloxy)octadecan-7-ol (R)-**6a**.* White solid; mp 56−58 °C; yield 80%; ^{1}H NMR (200 MHz, $CDCl_3$): δ 7.44−7.16 (5H, m, ArH), 4.50 (2H, s, $ArCH_2$), 3.66−3.52 (1H, m, C*H*OH), 3.47 (2H, t, *J* = 6.5 Hz, OCH_2), 1.75 (1H, s, OH), 1.69−1.54 (2H, m, 2 × C*H*H), 1.53−1.08 (28H, m, 28 × C*H*H), 0.89 (3H, t, *J* = 6.3 Hz, CH_3); ^{13}C NMR (50 MHz, $CDCl_3$): δ 138.5, 128.2, 127.5, 127.4, 72.8, 71.8, 70.3, 37.4, 37.3, 32.7, 31.9, 29.7, 29.6, 29.5, 29.4, 29.3, 26.1, 25.6, 25.5, 22.6, 14.1; $[\alpha]_D^{20}$ +1.2 (*c* 1.0, CH_2Cl_2); HRMS (ESI^+) *m*/*z*: calcd for $C_{25}H_{44}O_2Na^+$, 399.3234; $[M + Na]^+$ found, 399.3238.

*(S)-1-(Benzyloxy)octadecan-7-ol (S)-**6a**.* White solid; mp 56−58 °C; yield 83%; $[\alpha]_D^{20}$ −0.9 (*c* 1.0, CH_2Cl_2).

*(R)-1-(Benzyloxy)octadecan-10-ol (R)-**6b**.* White solid; mp 47−49 °C; yield 83%; ^{1}H NMR (200 MHz, $CDCl_3$): δ 7.38−7.20 (5H, m, ArH), 4.50 (2H, s, $ArCH_2$), 3.64−3.52 (1H, m, C*H*OH), 3.46 (2H, t, *J* = 6.6 Hz, OCH_2), 1.72−1.52 (3H, m, 2 × C*H*H, OH), 1.52−1.04 (28H, m, 28 × C*H*H), 0.88 (3H, t, *J* = 6.3 Hz, CH_3); ^{13}C NMR (50 MHz, $CDCl_3$): δ 138.7, 128.3, 127.6, 127.4, 72.8, 72.0, 70.5, 37.5, 31.9, 29.8, 29.7, 29.6, 29.5, 29.4, 29.3, 26.2, 25.6, 22.7, 14.1; $[\alpha]_D^{20}$ +1.5 (*c* 1.0, CH_2Cl_2); HRMS (ESI^+) *m*/*z*: calcd for $C_{25}H_{44}O_2Na^+$, 399.3234; $[M + Na]^+$ found, 399.3236.

*(S)-1-(Benzyloxy)octadecan-10-ol (S)-**6b**.* White solid; mp 47−49 °C; yield 82%; $[\alpha]_D^{20}$ −1.4 (*c* 1.0, CH_2Cl_2).

*(R)-1-(Benzyloxy)hexadecan-7-ol (R)-**6c**.* White solid; mp 50−53 °C; yield 71%; ^{1}H NMR (200 MHz, $CDCl_3$): δ 7.39−7.20 (5H, m, ArH), 4.50 (2H, s, $ArCH_2$), 3.63−3.52 (1H, m, C*H*OH), 3.46 (2H, t, *J* = 6.5 Hz, OCH_2), 1.73−1.51 (3H, m, 2 × C*H*H, OH), 1.51−1.03 (24H, m, 24 × C*H*H), 0.88 (3H, t, *J* = 5.3 Hz, CH_3); ^{13}C NMR (50 MHz, $CDCl_3$): δ 138.6, 128.3, 127.6, 127.4, 72.8, 71.9, 70.4, 37.5, 37.4, 31.9, 29.7, 29.6, 29.5, 29.3, 26.2, 25.6, 22.7, 14.1; $[\alpha]_D^{20}$ +1.3 (*c* 1.0, CH_2Cl_2); HRMS (ESI^+) *m*/*z*: calcd for $C_{23}H_{40}O_2Na^+$, 371.2921; $[M + Na]^+$ found, 371.2911.

*(S)-1-(Benzyloxy)hexadecan-7-ol (S)-**6c**.* White solid, mp 50−53 °C; yield 70%; $[\alpha]_D^{20}$ −1.8 (*c* 1.0, CH_2Cl_2).

*(R)-1-(Benzyloxy)hexadecan-10-ol (R)-**6d**.* White solid; mp 46−48 °C; yield 86%; ^{1}H NMR (200 MHz, $CDCl_3$): δ 7.42−7.18 (5H, m, ArH), 4.50 (2H, s, $ArCH_2$), 3.63−3.51 (1H, m, C*H*OH), 3.46 (2H, t, *J* = 6.6 Hz, OCH_2), 1.74−1.54 (3H, m, 2 × C*H*H, OH), 1.53−1.09 (24H, m, 24 × C*H*H), 0.89 (3H, t, *J* = 6.3 Hz, CH_3); ^{13}C NMR (50 MHz, $CDCl_3$): δ 138.6, 128.3, 127.5, 127.4, 72.8, 71.9, 70.4, 37.4, 31.8, 29.7, 29.6, 29.5, 29.4, 29.3, 26.1, 25.6, 22.6, 14.1; $[\alpha]_D^{20}$ +2.1 (*c* 1.0, CH_2Cl_2); HRMS (ESI^+) *m*/*z*: calcd for $C_{23}H_{40}O_2Na^+$, 371.2921; $[M + Na]^+$ found, 371.2909.

*(S)-1-(Benzyloxy)hexadecan-10-ol (S)-**6d**.* White solid; mp 46−48 °C; yield 87%; $[\alpha]_D^{20}$ −2.8 (*c* 1.0, CH_2Cl_2).

General Procedure for the Synthesis of Compounds (*R*)-7a−d and (*S*)-7a−d. To a flame-dried flask containing a solution of the secondary alcohol **6a−d** (1.00 mmol) in dry dichloromethane (10 mL) at 0 °C, dry pyridine (0.12 mL, 1.50 mmol) was added, followed by acetyl chloride (0.14 mL, 2.00 mmol). The mixture was then left to reach room temperature, and stirring was continued for 16 h. Then, a saturated aqueous solution of NH_4Cl (10 mL) was added, and the product was extracted with Et_2O (3 × 20 mL), dried over Na_2SO_4, filtered, and concentrated under reduced pressure. The acetyl protected product was purified by flash silica chromatography eluting with petroleum ether (bp 40−60 °C)/ethyl acetate 9/1.

*(R)-1-(Benzyloxy)octadecan-7-yl Acetate (R)-**7a**.* Yellowish oil; yield 89%; ^{1}H NMR (200 MHz, $CDCl_3$): δ 7.39−7.20 (5H, m, ArH), 4.92−4.78 (1H, m, CHOC═O), 4.50 (2H, s, $ArCH_2$), 3.45 (2H, t, *J* = 6.5 Hz, OCH_2), 2.03 (3H, s, CH_3C═O), 1.70−1.40 (8H, m, 8 × C*H*H), 1.40−1.14 (22H, m, 22 × C*H*H), 0.87 (3H, t, *J* = 6.0 Hz, CH_3); ^{13}C NMR (50 MHz, $CDCl_3$): δ 171.0, 138.6, 128.3, 127.6, 127.5, 74.4, 72.8, 70.4, 34.1, 34.0, 31.9, 29.6, 29.5, 29.3, 27.6, 26.1, 25.3, 25.2, 22.7, 21.3, 14.1; $[\alpha]_D^{20}$ +1.4 (*c* 1.0, $CHCl_3$); HRMS (ESI^+) *m*/*z*: calcd for $C_{27}H_{46}O_3Na^+$, 441.3339; $[M + Na]^+$ found, 441.3339.

*(S)-1-(Benzyloxy)octadecan-7-yl Acetate (S)-**7a**.* Yellowish oil; yield 98%; $[\alpha]_D^{20}$ −0.9 (*c* 1.0, $CHCl_3$).

*(R)-18-(Benzyloxy)octadecan-9-yl Acetate (R)-**7b**.* Yellowish oil; yield 94%; ^{1}H NMR (200 MHz, $CDCl_3$): δ 7.38−7.21 (5H, m, ArH), 4.91−4.79 (1H, m, CHOC═O), 4.50 (2H, s, $ArCH_2$), 3.46 (2H, t, *J* = 6.6 Hz, OCH_2), 2.04 (3H, s, CH_3C═O), 1.67−1.36 (8H, m, 8 × C*H*H), 1.36−1.13 (22H, m, 22 × C*H*H), 0.87 (3H, t, *J* = 6.1 Hz, CH_3); ^{13}C NMR (50 MHz, $CDCl_3$): δ 170.9, 138.7, 128.3, 127.6, 127.4, 74.4, 72.8, 70.5, 34.1, 31.8, 29.8, 29.5, 29.2, 26.2, 25.3, 22.6, 21.3, 14.1; $[\alpha]_D^{20}$ +1.1 (*c* 1.0, $CHCl_3$); HRMS (ESI^+) *m*/*z*: calcd for $C_{27}H_{46}O_3Na^+$, 441.3339; $[M + Na]^+$ found, 441.3340.

*(S)-18-(Benzyloxy)octadecan-9-yl Acetate (S)-**7b**.* Yellowish oil; yield 87%; $[\alpha]_D^{20}$ −0.9 (*c* 1.0, $CHCl_3$).

*(R)-1-(Benzyloxy)hexadecan-7-yl Acetate (R)-**7c**.* Yellowish oil; yield 96%; ^{1}H NMR (200 MHz, $CDCl_3$): δ 7.42−7.19 (5H, m, ArH), 4.92−4.79 (1H, m, CHOC═O), 4.50 (2H, s, $ArCH_2$), 3.46 (2H, t, *J* = 6.5 Hz, OCH_2), 2.03 (3H, s, CH_3C═O), 1.67−1.43 (6H, m, 6 × C*H*H), 1.43−1.04 (20H, m, 20 × C*H*H), 0.88 (3H, t, *J* = 6.3 Hz, CH_3); ^{13}C NMR (50 MHz, $CDCl_3$): δ 170.9, 138.6, 128.3, 127.6, 127.4, 74.4, 72.8, 70.4, 34.1, 34.0, 31.9, 29.7, 29.5, 29.3, 26.1, 25.3, 25.2, 22.7, 21.3, 14.1; $[\alpha]_D^{20}$ +1.3 (*c* 1.0, $CHCl_3$); HRMS (ESI^+) *m*/*z*: calcd for $C_{25}H_{42}O_3Na^+$, 413.3026; $[M + Na]^+$ found, 413.3022.

https://dx.doi.org/10.1021/acs.jmedchem.0c00844
J. Med. Chem. XXXX, XXX, XXX−XXX

*(S)-1-(Benzyloxy)hexadecan-7-yl Acetate (S)-**7c***. Yellowish oil; yield 95%; $[\alpha]_D^{20}$ −1.0 (*c* 1.0, $CHCl_3$).

*(R)-16-(Benzyloxy)hexadecan-7-yl Acetate (R)-**7d***. Yellowish oil; yield 92%; ^{1}H NMR (200 MHz, $CDCl_3$): δ 7.41−7.21 (5H, m, ArH), 4.91−4.79 (1H, m, CHOC═O), 4.50 (2H, s, $ArCH_2$), 3.46 (2H, t, *J* = 6.5 Hz, OCH_2), 2.03 (3H, s, CH_3C═O), 1.63−1.39 (6H, m, 6 × C*H*H), 1.39−1.11 (20H, m, 20 × C*H*H), 0.87 (3H, t, *J* = 6.2 Hz, CH_3); ^{13}C NMR (50 MHz, $CDCl_3$): δ 170.9, 138.7, 128.3, 127.6, 127.4, 74.4, 72.8, 70.5, 34.1, 31.7, 29.7, 29.5, 29.4, 29.2, 26.6, 26.1, 25.3, 22.6, 21.3, 14.0; $[\alpha]_D^{20}$ +1.8 (*c* 1.0, $CHCl_3$); HRMS (ESI^+) *m*/*z*: calcd for $C_{25}H_{42}O_3Na^+$, 413.3026; $[M + Na]^+$ found, 413.3016.

*(S)-16-(Benzyloxy)hexadecan-7-yl Acetate (S)-**7d***. Yellowish oil; yield 89%; $[\alpha]_D^{20}$ −2.0 (*c* 1.0, $CHCl_3$).

General Procedure for the Removal of Benzyl Group. A mixture of (*R*)- or (*S*)- **7a−d** (1.00 mmol) in MeOH (10 mL) and 10% palladium on activated charcoal was left stirring under a hydrogen atmosphere for 16 h. After filtration through a Celite pad, the solvent was evaporated to afford the desired alcohol without further purification.

*(R)-1-Hydroxyoctadecan-7-yl Acetate (R)-**8a***. Colorless oil; yield 88%; ^{1}H NMR (200 MHz, $CDCl_3$): δ 4.90−4.78 (1H, m, CHOC═O), 3.62 (2H, t, *J* = 6.5 Hz, CH_2OH), 2.03 (3H, s, CH_3C═O), 1.76 (1H, s, OH), 1.66−1.38 (8H, m, 8 × C*H*H), 1.38−1.16 (22H, m, 22 × C*H*H), 0.86 (3H, t, *J* = 6.4 Hz, CH_3); ^{13}C NMR (50 MHz, $CDCl_3$): δ 171.0, 74.3, 62.9, 34.1, 34.0, 32.6, 31.9, 29.6, 29.5, 29.3, 29.2, 25.6, 25.3, 25.2, 22.7, 21.3, 14.1; $[\alpha]_D^{20}$ +1.4 (*c* 1.0, $CHCl_3$); HRMS (ESI^+) *m*/*z*: calcd for $C_{20}H_{40}O_3Na^+$, 351.2870; $[M + Na]^+$ found, 351.2862.

*(S)-1-Hydroxyoctadecan-7-yl Acetate (S)-**8a***. Colorless oil; yield 72%; $[\alpha]_D^{20}$ −1.2 (*c* 1.0, $CHCl_3$).

*(R)-18-Hydroxyoctadecan-9-yl Acetate (R)-**8b***. Colorless oil; yield 87%; ^{1}H NMR (200 MHz, $CDCl_3$): δ 4.91−4.78 (1H, m, CHOC═O), 3.63 (2H, t, *J* = 6.5 Hz, CH_2OH), 2.03 (3H, s, CH_3C═O),1.69−1.40 (8H, m, 8 × C*H*H), 1.40−1.03 (23H, m, 22 × C*H*H, OH), 0.87 (3H, t, *J* = 6.4 Hz, CH_3); ^{13}C NMR (50 MHz, $CDCl_3$): δ 171.0, 74.4, 63.0, 34.1, 32.8, 31.8, 29.5, 29.4, 29.3, 29.2, 25.7, 25.3, 22.6, 21.3, 14.1; $[\alpha]_D^{20}$ +1.3 (*c* 1.0, $CHCl_3$); HRMS (ESI^+) *m*/*z*: calcd for $C_{20}H_{40}O_3Na^+$, 351.2870; $[M + Na]^+$ found, 351.2875.

*(S)-18-Hydroxyoctadecan-9-yl Acetate (S)-**8b***. Colorless oil; yield 78%; $[\alpha]_D^{20}$ −1.6 (*c* 1.0, $CHCl_3$).

*(R)-1-Hydroxyhexadecan-7-yl Acetate (R)-**8c***. Colorless oil; yield 99%; ^{1}H NMR (200 MHz, $CDCl_3$): δ 4.93−4.76 (1H, m, CHOC═O), 3.63 (2H, t, *J* = 6.4 Hz, CH_2OH), 2.03 (3H, s, CH_3C═O), 1.65−1.43 (7H, m, 6 × C*H*H, OH), 1.43−1.11 (20H, m, 20 × C*H*H), 0.87 (3H, t, *J* = 6.0 Hz, CH_3); ^{13}C NMR (50 MHz, $CDCl_3$): δ 171.0, 74.3, 62.9, 34.1, 34.0, 32.6, 31.9, 29.5, 29.3, 29.2, 25.6, 25.3, 25.2, 22.7, 21.3, 14.1; $[\alpha]_D^{20}$ +1.1 (*c* 0.5, $CHCl_3$); HRMS (ESI^+) *m*/*z*: calcd for $C_{18}H_{36}O_3Na^+$, 323.2557; $[M + Na]^+$ found, 323.2550.

*(S)-1-Hydroxyhexadecan-7-yl Acetate (S)-**8c***. Colorless oil; yield 97%; $[\alpha]_D^{20}$ −1.2, (*c* 0.5, $CHCl_3$).

*(R)-16-Hydroxyhexadecan-7-yl Acetate (R)-**8d***. Colorless oil; yield 99%; ^{1}H NMR (200 MHz, $CDCl_3$): δ 4.90−4.78 (1H, m, CHOC═O), 3.62 (2H, t, *J* = 6.5 Hz, CH_2OH), 2.02 (3H, s, CH_3C═O), 1.63−1.41 (7H, m, 6 × C*H*H, OH), 1.41−1.05 (20H, m, 20 × C*H*H), 0.86 (3H, t, *J* = 6.4 Hz, CH_3); ^{13}C NMR (50 MHz, $CDCl_3$): δ 171.0, 74.4, 63.0, 34.1, 32.7, 31.7, 29.4, 29.3, 29.2, 25.7, 25.2, 22.6, 21.3, 14.0; $[\alpha]_D^{20}$ +2.7 (*c* 1.0, $CHCl_3$); HRMS (ESI^+) *m*/*z*: calcd for $C_{18}H_{36}O_3Na^+$, 323.2557; $[M + Na]^+$ found, 323.2552.

*(S)-16-Hydroxyhexadecan-7-yl Acetate (S)-**8d***. Colorless oil; yield 86%; $[\alpha]_D^{20}$ −2.2 (*c* 1.0, $CHCl_3$).

General Procedure for the Oxidation of Alcohols to Compounds (*R*)-9a−d and (*S*)-9a−d. To a solution of alcohol **8a−d** (1 mmol) in acetone (10 mL) at 0 °C, the Jones reagent (2 M, 1.5 mL, 3 mmol) was added dropwise at 0 °C. The reaction was left under stirring at 0 °C for 1 h. Then, a saturated solution of $NaHSO_3$ (10 mL) was added at room temperature. The mixture was extracted with Et_2O (3 × 20 mL), washed with brine (1 × 50 mL), dried over Na_2SO_4, filtered, and concentrated under reduced pressure. The acids were purified by flash chromatography eluting with petroleum ether (bp 40−60 °C)/ethyl acetate 6/4.

*(R)-7-Acetoxyoctadecanoic Acid (R)-**9a***. Colorless oil; yield 82%; ^{1}H NMR (200 MHz, $CDCl_3$): δ 4.91−4.78 (1H, m, CHOC═O), 2.34 (2H, t, *J* = 7.3 Hz, CH_2COOH), 2.03 (3H, s, CH_3C═O), 1.74−1.43 (6H, m, 6 × C*H*H), 1.43−0.99 (22H, m, 22 × C*H*H) 0.87 (3H, t, *J* = 6.1 Hz, CH_3); ^{13}C NMR (50 MHz, $CDCl_3$): δ 179.5, 171.0, 74.3, 34.1, 33.9, 31.9, 29.6, 29.5, 29.3, 28.9, 25.3, 24.9, 24.5, 22.7, 21.3, 14.1; $[\alpha]_D^{20}$ +1.4 (*c* 0.5, $CHCl_3$); HRMS (ESI^-) *m*/*z*: calcd for $C_{20}H_{37}O_4^-$, 341.2697; $[M - H]^-$ found, 341.2691.

*(S)-7-Acetoxyoctadecanoic Acid (S)-**9a***. Colorless oil; yield 77%; $[\alpha]_D^{20}$ −1.0 (*c* 0.5, $CHCl_3$).

*(R)-10-Acetoxyoctadecanoic Acid (R)-**9b***. Colorless oil; yield 92%; ^{1}H NMR (200 MHz, $CDCl_3$): δ 4.92−4.78 (1H, m, CHOC═O), 2.34 (2H, t, *J* = 7.4 Hz, CH_2COOH), 2.03 (3H, s, CH_3C═O), 1.72−1.42 (6H, m, 6 × C*H*H), 1.42−1.09 (22H, m, 22 × C*H*H) 0.87 (3H, t, *J* = 5.5 Hz, CH_3); ^{13}C NMR (50 MHz, $CDCl_3$): δ 179.7, 171.0, 74.4, 34.1, 34.0, 31.8, 29.5, 29.4, 29.3, 29.2, 29.1, 29.0, 25.3, 24.6, 22.6, 21.3, 14.1; $[\alpha]_D^{20}$ +1.4 (*c* 0.5, $CHCl_3$); HRMS (ESI^-) *m*/*z*: calcd for $C_{20}H_{37}O_4^-$, 341.2697; $[M - H]^-$ found, 341.2690.

*(S)-10-Acetoxyoctadecanoic Acid (S)-**9b***. Colorless oil; yield 93%; $[\alpha]_D^{20}$ −1.2 (*c* 0.5, $CHCl_3$).

*(R)-7-Acetoxyhexadecanoic Acid (R)-**9c***. Colorless oil; yield 96%; ^{1}H NMR (200 MHz, $CDCl_3$): δ 4.90−4.78 (1H, m, CHOC═O), 2.34 (2H, t, *J* = 7.4 Hz, CH_2COOH), 2.03 (3H, s, CH_3C═O), 1.70−1.42 (6H, m, 6 × C*H*H), 1.42−1.04 (18H, m, 18 × C*H*H) 0.87 (3H, t, *J* = 6.4 Hz, CH_3); ^{13}C NMR (50 MHz, $CDCl_3$): δ 179.6, 171.0, 74.3, 34.1, 33.9, 31.9, 29.5, 29.3, 28.9, 25.3, 24.9, 24.5, 22.7, 21.3, 14.1; $[\alpha]_D^{20}$ +3.0 (*c* 0.5, $CHCl_3$); HRMS (ESI^+) *m*/*z*: calcd for $C_{18}H_{34}O_4Na^+$, 337.2349; $[M + Na]^+$ found, 337.2351.

*(S)-7-Acetoxyhexadecanoic Acid (S)-**9c***. Colorless oil; yield 92%; $[\alpha]_D^{20}$ −2.5 (*c* 0.5, $CHCl_3$).

*(R)-10-Acetoxyhexadecanoic Acid (R)-**9d***. Colorless oil; yield 83%; ^{1}H NMR (200 MHz, $CDCl_3$): δ 4.90−4.78 (1H, m, CHOC═O), 2.33 (2H, t, *J* = 7.4 Hz, CH_2COOH), 2.03 (3H, s, CH_3C═O), 1.69−1.42 (6H, m, 6 × C*H*H), 1.42−1.11 (18 H, m, 18 × C*H*H) 0.86 (3H, t, *J* = 6.0 Hz, CH_3); ^{13}C NMR (50 MHz, $CDCl_3$): δ 180.0, 171.0, 74.4, 34.1, 34.0, 31.7, 29.4, 29.3, 29.2, 29.1, 29.0, 25.2, 24.6, 22.6, 21.3, 14.0; $[\alpha]_D^{20}$ +1.1 (*c* 1.0, $CHCl_3$); HRMS (ESI^+) *m*/*z*: calcd for $C_{18}H_{34}O_4Na^+$, 337.2349; $[M + Na]^+$ found, 337.2343.

*(S)-10-Acetoxyhexadecanoic Acid (S)-**9d***. Colorless oil; yield 82%; $[\alpha]_D^{20}$ −1.3 (*c* 1.0, $CHCl_3$)

General Procedure for the Removal of the Acetyl Group. Compounds **9a−d** (1 mmol) were dissolved in a mixture of THF and H_2O (1:1, 5 mL), followed by the addition of LiOH (96 mg, 4 mmol), and the reaction mixture was left under stirring at room temperature for 16 h. After the addition of a solution of HCl 1 N (10 mL) to pH 1, the mixture was extracted with Et_2O (3 × 10 mL), washed with brine (1 × 30 mL), dried over Na_2SO_4, filtered, and evaporated under reduced pressure. The hydroxy fatty acids were purified by silica gel flash chromatography eluting with petroleum ether (bp 40−60 °C)/ethyl acetate 2/8.

*(R)-7-Hydroxyoctadecanoic Acid (R)-**10a***. White solid; mp 72−75 °C; yield 72%; ^{1}H NMR (400 MHz, $CDCl_3$): δ 6.22 (1H, br s, COOH), 3.68−3.50 (1H, m, C*H*OH), 2.33 (2H, t, *J* = 7.4 Hz, CH_2COOH), 1.81−1.52 (3H, m, 2 × C*H*H, OH), 1.52−1.10 (26H, m, 26 × C*H*H), 0.87 (3H, t, *J* = 6.4 Hz, CH_3); ^{13}C NMR (100 MHz, $CDCl_3$): δ 179.2, 72.0, 37.4, 37.0, 33.9, 31.9, 29.7, 29.6, 29.3, 29.1, 25.6, 25.2, 24.6, 22.7, 14.1; $[\alpha]_D^{20}$ −3.6 (*c* 1.0, $CHCl_3$); HRMS (ESI^-) *m*/*z*: calcd for $C_{18}H_{35}O_3^-$, 299.2592; $[M - H]^-$ found, 299.2592.

*(S)-7-Hydroxyoctadecanoic Acid (S)-**10a***. White solid; mp 72−75 °C; yield 73%; $[\alpha]_D^{20}$ +4.5 (*c* 1.0, $CHCl_3$).

*(R)-10-Hydroxyoctadecanoic Acid (R)-**10b***. White solid; mp 82−84 °C; yield 69%; ^{1}H NMR (400 MHz, $CDCl_3$): δ 3.63−3.54 (1H, m, C*H*OH), 2.34 (2H, t, *J* = 7.5 Hz, CH_2COOH), 1.70−1.52 (3H, m, 2 × C*H*H, OH), 1.52−1.15 (26H, m, 26 × C*H*H), 0.88 (3H, t, *J* = 6.7 Hz, CH_3); ^{13}C NMR (100 MHz, $CDCl_3$): δ 179.0, 72.1, 37.5, 37.4, 33.9, 31.9, 29.7, 29.6, 29.3, 29.1, 29.0, 25.6, 24.6, 22.7, 14.1; $[\alpha]_D^{20}$ −2.4 (*c* 1.0, $CHCl_3$); HRMS (ESI^-) *m*/*z*: calcd for $C_{18}H_{35}O_3^-$, 299.2592; $[M - H]^-$ found, 299.2591.

*(S)-10-Hydroxyoctadecanoic Acid (S)-**10b***. White solid; mp 82−84 °C; yield 65%; $[\alpha]_D^{20}$ +2.8 (*c* 1.0, $CHCl_3$).

https://dx.doi.org/10.1021/acs.jmedchem.0c00844
J. Med. Chem. XXXX, XXX, XXX−XXX

*(R)-7-Hydroxyhexadecanoic Acid (R)-**10c***. White solid; mp 60−62 °C; yield 67%; ^{1}H NMR (400 MHz, $CDCl_3$): δ 5.29, (1H, br s, COOH), 3.66−3.53 (1H, m, C*H*OH), 2.34 (2H, t, J = 7.4 Hz, CH_2COOH), 1.72−1.56 (2H, m, 2 × C*H*H), 1.55−1.09 (23H, m, 22 × C*H*H, OH), 0.88 (3H, t, J = 6.7 Hz, CH_3); ^{13}C NMR (100 MHz, $CDCl_3$): δ 179.1, 72.0, 37.5, 37.1, 33.9, 31.9, 29.7, 29.6, 29.3, 29.1, 25.6, 25.2, 24.6, 22.7, 14.1; $[\alpha]_D^{20}$ −2.6 (c 1.0, $CHCl_3$); HRMS (ESI^-) m/z: calcd for $C_{16}H_{31}O_3^-$, 271.2279; $[M - H]^-$ found, 271.2266.

*(S)-7-Hydroxyhexadecanoic Acid (S)-**10c***. White solid; mp 60−62 °C; yield 65%; $[\alpha]_D^{20}$ +3.0 (c 1.0, $CHCl_3$).

*(R)-10-Hydroxyhexadecanoic Acid (R)-**10d***. White solid; mp 64−67 °C; yield 77%; ^{1}H NMR (400 MHz, $CDCl_3$): δ 6.61 (1H, br s, COOH), 3.67−3.52 (1H, m, C*H*OH), 2.31 (2H, t, J = 7.5 Hz, CH_2COOH), 1.69−1.53 (2H, m, 2 × C*H*H), 1.53−1.09 (23H, m, 22 × C*H*H, OH), 0.87 (3H, t, J = 6.7 Hz, CH_3); ^{13}C NMR (100 MHz, $CDCl_3$): δ 179.4, 72.1, 37.3, 37.2, 34.0, 31.8, 29.5, 29.3, 29.1, 29.0, 25.5, 24.6, 22.6, 14.0; $[\alpha]_D^{20}$ −3.0 (c 1.0, $CHCl_3$); HRMS (ESI^-) m/z: calcd for $C_{16}H_{31}O_3^-$, 271.2279; $[M - H]^-$ found, 271.2269.

*(S)-10-Hydroxyhexadecanoic Acid (S)-**10d***. White solid; mp 64−67 °C; yield 83%; $[\alpha]_D^{20}$ +3.2 (c 1.0, $CHCl_3$).

Suspect Screening Analysis and Determination of SHFAs. LC−MS/MS measurements were performed with an ABSciex Triple TOF 4600 combined with a micro-LC Eksigent and an autosampler set at 5 °C and a thermostated column compartment. Electrospray ionization (ESI) in negative mode was used for all the MS experiments. The data acquisition method consisted of a TOF-MS full scan m/z 50−850 and several information dependent acquisition-TOF-MS/MS product ion scans using 40 V collision energy with 15 V collision energy spread used for each candidate ion in each data acquisition cycle (1091). A Halo C18 2.7 μm, 90 Å, 0.5 × 50 mm column from Eksigent was used, and the mobile phase consisted of a gradient (A: acetonitrile/0.01% formic acid/isopropanol 80/20 v/v; B: H_2O/0.01% formic acid). The data acquisition was carried out with MultiQuant 3.0.2 and PeakView 2.1 from AB SCIEX. EICs were obtained with the use of MultiQuant 3.0.2, which created the base peak chromatograms for the masses that achieve a 0.01 mass accuracy width. The relative tolerance of the retention time was set within a margin of ±2.5%. Ten samples of human plasma and 10 samples of cow milk were analyzed by LC−HRMS. Ten brand products of fresh (pasteurized) whole cow milk (fat content 3.5−3.7%) were collected from the local market in Athens, Greece.

MTT Assay. All four cells lines used were cultured as described. After 24 h, the medium was changed to one containing the desired compounds at selected concentrations, including control samples with the equivalent vehicle amount. HFAs, FAs, and FAHFAs were dissolved in DMSO to prepare a stock solution of 10 mM. The final solutions were prepared by appropriate dilution of the stock solution in media maintaining a final 0.5% DMSO content. A triplicate for each condition was always executed in the same plate. Following 72 h, MTT was added at a final concentration of 0.25 mg/mL and incubated for 3 h. The medium was removed, and DMSO was added to dissolve the formazan crystals. The formazan absorbance was measured at 570 nm using an ELISA Plate reader (ELX800, BIOTEC), while the background absorbance was measured at 690 nm.

Cell Growth Inhibition Analysis. Data analysis was performed using Microsoft Excel (Office Professional Plus 2016). The 690 nm background absorbance was subtracted from the 570 nm values, and the average of the three repeats per condition was calculated. The data set was normalized to DMSO control cells as 100% survival value. The curves were generated using GraphPad Prism version 6.01, and the IC_{50} values were calculated from the resultant plots. Two-way ANOVA statistical analysis with multiple comparisons was performed on this data set comparing the various concentrations of the compounds investigated to DMSO control.

Image Data Analysis. Cell nuclei were identified in all samples using DAPI staining. pH3 and casp3 positive nuclei were overlaid onto the DAPI images and quantified using ImageJ (NIH). Values were normalized to DMSO control conditions using Microsoft Excel, while graphs were created using GraphPad Prism 6.01. One-way ANOVA statistical analysis was performed for each separate immunostaining set comparing all conditions to control.

RNA Extraction and Real-Time RT-qPCR Analysis. Total RNA was isolated by TRI reagent solution (AM9738, Ambion/RNA, Life Technologies), according to the manufacturer's instructions, followed by treatment with RQ1 DNase (Promega, Madison, WI, USA). RNA concentration and purity were measured by Nanodrop 2000c (Thermo), and 1.5 μg was used for cDNA synthesis using the SuperScript First-Strand Synthesis System (Invitrogen, Carlsbad, USA) together with random hexamer primers. Quantitative real-time RT-qPCR analysis was performed in a LightCycler 96 Instrument (Roche). Measured values were normalized using beta actin mRNA levels as internal references. Primers used for real-time RT-qPCR are shown in Table 1S.

Immunoblotting. Total protein was isolated from treated and untreated A549 cell with lysis buffer RIPA. The homogenates were centrifuged at 17,000g for 15 min at 4 °C. The supernatants were collected, and protein concentration was measured with Bradford protein assay (Bio-Rad protein assay). Protein samples (35 μg) were loaded each time into sodium dodecyl sulfate-polyacrylamide gel electrophoresis gels and transferred to nitrocellulose membranes (Amersham) using the semidry transfer system (Bio-Rad). The membranes were blocked with BSA (AppliChem, A1391) 5% dissolved in Tris-buffered saline (1×) containing 0.1% Tween 20 for 1 h at r.t. The membranes were incubated with primary antibodies at 4 °C overnight, followed by secondary antibodies for 1.30 h at r.t. The primary antibodies in the Western blot were rabbit anti-phospho-STAT3 (Cell Signaling, 9145) (1:1000 dilution), rabbit anti-STAT3 (Santa Cruz, sc-482) (1:1000 dilution), and mouse anti-beta actin (Sigma, A5441) (1:20,000 dilution). The secondary antibodies were rabbit anti-mouse IgG (Sigma, A9044) (1:20000 dilution) and goat anti-rabbit IgG (Sigma, A6154) (1:10000 dilution) IgGs.

Cell Culture and Immunostaining. A549 cells were cultured in a 37 °C humidified incubator with 5% CO_2 cells in DMEM (4.5 g/L glucose, Biosera) supplemented with 10% (v/v) heat-inactivated FBS (Biosera) and pen-strep (100 and 100 μg/mL, respectively; Invitrogen). For the immunostaining experiments, A549 cells were cultured onto poly-L-lysine (Sigma)-coated coverslips in 24-well plates. After treatment, the cells were fixed on the coverslips with 4% PFA (paraformaldehyde) and prepared for immunostaining experiments. The coverslips were blocked with 5% FBS dissolved in phosphate-buffered saline (PBS) (1×) containing 0.1% Triton X-100 for 1 h at r.t. Next, they were incubated with primary antibodies at 4 °C overnight, followed by secondary antibodies for 1 h at r.t. Finally, they were incubated with DAPI diluted in 1× PBS for 10 min at r.t., followed by mounting with MOWIOL. The primary antibodies in the immunofluorescence were rabbit anti-phospho-Histone 3 (Abcam, Ab5176) (1:600 dilution) and rabbit anticleaved caspase 3 (Cell Signaling, 9661) (1:800 dilution). The secondary antibody was donkey anti-rabbit 488 (AlexaFluor). Immunostained cells were imaged on an upright microscope (Leica).

TUNEL Analyses. HFAs and PAHSA were dissolved in DMSO to prepare a stock solution. Additional dilutions were made, if needed, in DMSO and the final added volume (to achieve any final concentration) was 1 μL in 1000 μL media. Thus, the final concentration of DMSO was always 1:1000 (v/v) or 0.10%. INS-1 cells were cultured in RPMI (containing 10% fetal calf serum, 2 mmo/L glutamine, 1% of 100× penicillin/streptomycin, 10 mM HEPES, 1 mM sodium pyruvate) at 37 °C under an atmosphere of 5% CO_2/95% air for up to 24 h until ca 70% confluency was achieved. The cells were treated with either 1 or 10 μM of each SHFAs for 1 h, prior to exposures to vehicle (DMSO, 1 μL/mL) alone or CTK IL-1β (20 ng/mL, R&D systems, 501-RL) + IFNγ (200 ng/mL, R&D systems, 585-IF) for 16 h. The cells were then harvested and washed twice with ice-cold PBS, immobilized on slides by cytospin, and fixed with 4% paraformaldehyde (in PBS, pH 7.4, for 1 h at r.t.). The INS-1 cells were then washed with PBS and incubated in permeabilization solution (0.1% Triton X-100 in 0.1% sodium citrate in PBS for 30 min at r.t.). The permeabilization solution was then removed and processed for TUNEL analyses using the In Situ Cell Death

https://dx.doi.org/10.1021/acs.jmedchem.0c00844
J. Med. Chem. XXXX, XXX, XXX−XXX

Detection Kit, Fluorescein (catalog number 11684795910; Roche Applied Science, Mannheim, Germany), as described.[47] The cells were washed with PBS and counterstained with 1 μg/mL DAPI in PBS for 10 min to identify cellular nuclei. Incidence of apoptosis was assessed under a fluorescence microscope using a FITC filter. Cells with TUNEL-positive nuclei were considered apoptotic. DAPI staining was used to determine the total number of INS-1 cells in a field. A minimum of three fields per slide was used to calculate the percentage of apoptotic islet cells.

Statistics. Comparisons between two data groups (with $n \geq 3$ independent experiments) were analyzed using a Student's t-test. Values of <0.05 were considered significant and are indicated in the graphs as $*p < 0.05$, $**p < 0.01$, or $***p < 0.001$. All data represent the mean ± SEM ($n \geq 3$).

■ ASSOCIATED CONTENT

Supporting Information

The Supporting Information is available free of charge at https://pubs.acs.org/doi/10.1021/acs.jmedchem.0c00844.

Cell growth inhibitory potency of HSAs and HPAs on human cancer cell line U87-MG, 2-way ANOVA statistical analysis, effect of 7RHSA and 9RSHA on cell death and apoptosis of SF268 cells, primers used for real-time RT-qPCR, and ^{1}H NMR and ^{13}C NMR spectra of the compounds synthesized (PDF)

Molecular formula strings and inhibition data (CSV)

■ AUTHOR INFORMATION

Corresponding Author

George Kokotos − *Department of Chemistry, National and Kapodistrian University of Athens, Athens 15771, Greece;* orcid.org/0000-0003-3753-7082; Phone: +30 210 7274462; Email: gkokotos@chem.uoa.gr; Fax: +30 210 7274761

Authors

Maroula G. Kokotou − *Department of Chemistry, National and Kapodistrian University of Athens, Athens 15771, Greece*

Alexandros C. Kokotos − *Center of Basic Research, Biomedical Research Foundation of the Academy of Athens, Athens 11527, Greece*

Dimitrios Gkikas − *Center of Basic Research, Biomedical Research Foundation of the Academy of Athens, Athens 11527, Greece*

Olga G. Mountanea − *Department of Chemistry, National and Kapodistrian University of Athens, Athens 15771, Greece*

Christiana Mantzourani − *Department of Chemistry, National and Kapodistrian University of Athens, Athens 15771, Greece*

Abdulaziz Almutairi − *Department of Cell, Developmental, and Integrative Biology and Comprehensive Diabetes Center, University of Alabama at Birmingham, Birmingham, Alabama 35294, United States*

Xiaoyong Lei − *Department of Cell, Developmental, and Integrative Biology and Comprehensive Diabetes Center, University of Alabama at Birmingham, Birmingham, Alabama 35294, United States*

Sasanka Ramanadham − *Department of Cell, Developmental, and Integrative Biology and Comprehensive Diabetes Center, University of Alabama at Birmingham, Birmingham, Alabama 35294, United States*

Panagiotis K. Politis − *Center of Basic Research, Biomedical Research Foundation of the Academy of Athens, Athens 11527, Greece*

Complete contact information is available at: https://pubs.acs.org/10.1021/acs.jmedchem.0c00844

Author Contributions

#A.C.K., D.G., O.G.M. authors contributed equally.

Notes

The authors declare no competing financial interest.

■ ACKNOWLEDGMENTS

The research presented was carried out within the framework of a Stavros Niarchos Foundation grant to the National and Kapodistrian University of Athens (G.K.). This work was partially supported by a Fondation Sante grant and the Hellenic Foundation for Research and Innovation (H.F.R.I.) under the "First Call for H.F.R.I. Research Projects to support Faculty members and Researchers and the procurement of high-cost research equipment grant" (Project Number: 1782) (P.K.P.) and by NIH Grants R01DK-69455 and R01 DK110292 (S.R.). The research work was supported by the Hellenic Foundation for Research and Innovation (HFRI) under the HFRI PhD Fellowship grant (Fellowship Number: 1338) (O.M).

■ ABBREVIATIONS

Casp3, activated caspase 3; CTK, cytokines; DMSO, dimethyl sulfoxide; ee, enantiomeric excess; EICs, extracted ion chromatograms; FAHFAs, fatty acid esters of hydroxy fatty acids; HCA, hydroxycapric acid; 2HFAs, 2-hydroxy fatty acids; 3HFAs, 3-hydroxy fatty acids; HLA, hydroxylauric acid; HMA, hydroxymyristic acid; HPA, hydroxypalmitic acid; HRMS, high-resolution mass spectrometry; HSA, hydroxystearic acid; PAHSA, palmitic acid ester of 9-hydroxystearic acid; PCC, pyridinium chlorochromate; pH3, phosphorylated histone H3; p-STAT3, phosphorylated STAT3; SHFAs, saturated hydroxy fatty acids; SPM, specialized proresolving mediators; STAT3, transcription regulator signal transducer and activator of transcription 3; THF, tetrahydrofuran

■ REFERENCES

(1) *Bioactive Lipids*; Kokotos, G., Nicolaou, A., Eds.; The Oily Press: Bridgewater, England, 2004.

(2) Serhan, C. N.; Hong, S.; Gronert, K.; Colgan, S. P.; Devchand, P. R.; Mirick, G.; Moussignac, R.-L. Resolvins: A family of bioactive products of omega-3 fatty acid transformation circuits initiated by aspirin treatment that counter proinflammation signals. *J. Exp. Med.* **2002**, *196*, 1025−1037.

(3) Serhan, C. N.; Petasis, N. A. Resolvins and protectins in inflammation resolution. *Chem. Rev.* **2011**, *111*, 5922−5943.

(4) Serhan, C. N. Pro-resolving lipid mediators are leads for resolution physiology. *Nature* **2014**, *510*, 92−101.

(5) Hama, H. Fatty acid 2-hydroxylation in mammalian sphingolipid biology. *Biochim. Biophys. Acta, Mol. Cell Biol. Lipids* **2010**, *1801*, 405−414.

(6) Raetz, C. R. H.; Whitfield, C. Lipopolysaccharide endotoxins. *Annu. Rev. Biochem.* **2002**, *71*, 635−700.

(7) Offermanns, S. Free fatty acid (FFA) and carboxylic acid (HCA) receptor. *Annu. Rev. Pharmacol. Toxicol.* **2014**, *54*, 407−434.

(8) Suzuki, M.; Takaishi, S.; Nagasaki, M.; Onozawa, Y.; Iino, I.; Maeda, H.; Komai, T.; Oda, T. Medium-chain fatty acid-sensing receptor, GPR84, is a proinflammatory receptor. *J. Biol. Chem.* **2013**, *288*, 10684−10691.

(9) Köse, M.; Pillaiyar, T.; Namasivayam, V.; De Filippo, E.; Sylvester, K.; Ulven, T.; von Kügelgen, I.; Müller, C. E. An agonist radioligand for the proinflammatory lipid-activated G protein-coupled

receptor GPR84 providing structural insights. *J. Med. Chem.* **2020**, *63*, 2391−2410.
(10) Yore, M. M.; Syed, I.; Moraes-Vieira, P. M.; Zhang, T.; Herman, M. A.; Homan, E. A.; Patel, R. T.; Lee, J.; Chen, S.; Peroni, O. D.; Dhaneshwar, A. S.; Hammarstedt, A.; Smith, U.; McGraw, T. E.; Saghatelian, A.; Kahn, B. B. Discovery of a class of endogenous mammalian lipids with anti-diabetic and anti-inflammatory effects. *Cell* **2014**, *159*, 318−332.
(11) Moraes-Vieira, P. M.; Saghatelian, A.; Kahn, B. B. GLUT4 expression in adipocytes regulates de novo lipogenesis and levels of a novel class of lipids with antidiabetic and anti-inflammatory effects. *Diabetes* **2016**, *65*, 1808−1815.
(12) Syed, I.; Lee, J.; Moraes-Vieira, P. M.; Donaldson, C. J.; Sontheimer, A.; Aryal, P.; Wellenstein, K.; Kolar, M. J.; Nelson, A. T.; Siegel, D.; Mokrosinski, J.; Farooqi, I. S.; Zhao, J. J.; Yore, M. M.; Peroni, O. D.; Saghatelian, A.; Kahn, B. B. Palmitic acid hydroxystearic acids activate GPR40, which is involved in their beneficial effects on glucose homeostasis. *Cell Metab.* **2018**, *27*, 419−427.
(13) Pflimlin, E.; Bielohuby, M.; Korn, M.; Breitschopf, K.; Löhn, M.; Wohlfart, P.; Konkar, A.; Podeschwa, M.; Bärenz, F.; Pfenninger, A.; Schwahn, U.; Opatz, T.; Reimann, M.; Petry, S.; Tennagels, N. Acute and repeated treatment with 5-PAHSA or 9-PAHSA isomers does not improve glucose control in mice. *Cell Metab.* **2018**, *28*, 217−227.
(14) Kuda, O. On the complexity of PAHSA research. *Cell Metab.* **2018**, *28*, 541−542.
(15) Lee, J.; Moraes-Vieira, P. M.; Aryal, P.; Yee, E. U.; Vickers, C.; Parnas, O.; Donaldson, C. J.; Saghatelian, A.; Kahn, B. B.; Kahn, B. B. Branched fatty acid esters of hydroxy fatty acids (FAHFAs) protect against colitis by regulating gut innate and adaptive immune responses. *J. Biol. Chem.* **2016**, *291*, 22207−22217.
(16) Vihervaara, T.; Suoniemi, M.; Laaksonen, R. Lipidomics in drug discovery. *Drug Discov. Today* **2014**, *19*, 164−170.
(17) Watrous, J. D.; Niiranen, T. J.; Lagerborg, K. A.; Henglin, M.; Xu, Y. J.; Rong, J.; Sharma, S.; Vasan, R. S.; Larson, M. G.; Armando, A.; Mora, S.; Quehenberger, O.; Dennis, E. A.; Cheng, S.; Jain, M. Directed non-targeted mass spectrometry and chemical networking for discovery of eicosanoids and related oxylipins. *Cell Chem. Biol.* **2019**, *26*, 433.
(18) Seo, C.; Yoon, J.; Rhee, Y.; Kim, J.-J.; Nam, S.-J.; Lee, W.; Lee, G.; Yee, S.-T.; Paik, M.-J. Simultaneous analysis of seven 2-hydroxy fatty acids as tert-butyldimethylsilyl derivatives in plasma by gas chromatography−mass spectrometry. *Biomed. Chromatogr.* **2015**, *29*, 156−160.
(19) Jones, P. M.; Bennett, M. J. Clinical applications of 3-hydroxy fatty acid analysis by gas chromatography−mass spectrometry. *Biochim. Biophys. Acta* **2011**, *1811*, 657−662.
(20) Jenske, R.; Vetter, W. Enantioselective analysis of 2- and 3-hydroxy fatty acids in food samples. *J. Agric. Food Chem.* **2008**, *56*, 11578−11583.
(21) Jenske, R.; Vetter, W. Concentrations of medium-chain 2- and 3-hydroxy fatty acids in foodstuffs. *Food Chem.* **2009**, *114*, 1122−1129.
(22) Márquez-Ruiz, G.; Rodríguez-Pino, V.; de la Fuente, M. A. Determination of 10-hydroxystearic, 10-ketostearic, 8-hydroxypalmitic, and 8- ketopalmitic acids in milk fat by solid-phase extraction plus gas chromatography-mass spectrometry. *J. Dairy Sci.* **2011**, *94*, 4810−4819.
(23) Mountanea, O. G.; Limnios, D.; Kokotou, M. G.; Bourboula, A.; Kokotos, G. Asymmetric synthesis of saturated hydroxy fatty acids and fatty acid esters of hydroxy fatty acids. *Eur. J. Org. Chem.* **2019**, 2010−2019.
(24) Cavalli, G.; Casali, E.; Spisni, A.; Masotti, L. Identification of the peroxidation product hydroxystearic acid in Lewis lung carcinoma cells. *Biochem. Biophys. Res. Commun.* **1991**, *178*, 1260−1265.
(25) Calonghi, N.; Cappadone, C.; Pagnotta, E.; Farruggia, G.; Buontempo, F.; Boga, C.; Brusa, G. L.; Santucci, M. A.; Masotti, L. 9-Hydroxystearic acid upregulates p21WAF1 in HT29 cancer cells. *Biochem. Biophys. Res. Commun.* **2004**, *314*, 138−142.
(26) Calonghi, N.; Cappadone, C.; Pagnotta, E.; Boga, C.; Bertucci, C.; Fiori, J.; Tasco, G.; Casadio, R.; Masotti, L. Histone deacetylase 1: A target of 9-hydroxystearic acid in the inhibition of cell growth in human colon cancer. *J. Lipid Res.* **2005**, *46*, 1596−1603.
(27) Calonghi, N.; Pagnotta, E.; Parolin, C.; Tognoli, C.; Boga, C.; Masotti, L. 9-Hydroxystearic acid interferes with EGF signaling in a human colon adenocarcinoma. *Biochem. Biophys. Res. Commun.* **2006**, *342*, 585−588.
(28) Calonghi, N.; Pagnotta, E.; Parolin, C.; Molinari, C.; Boga, C.; Dal Piaz, F.; Brusa, G. L.; Santucci, M. A.; Masotti, L. Modulation of apoptotic signalling by 9-hydroxystearic acid in osteosarcoma cells. *Biochim. Biophys. Acta* **2007**, *1771*, 139−146.
(29) van Meerloo, J.; Kaspers, G. J. L.; Cloos, J. Cell sensitivity assays: The MTT assay. *Methods Mol. Biol.* **2011**, *731*, 237−245.
(30) Foskolou, I. P.; Stellas, D.; Rozani, I.; Lavigne, M. D.; Politis, P. K. Prox1 suppresses the proliferation of neuroblastoma cells via a dual action in p27-Kip1 and Cdc25A. *Oncogene* **2013**, *32*, 947−960.
(31) Stergiopoulos, A.; Politis, P. K. Nuclear receptor NR5A2 controls neural stem cell fate decisions during development. *Nat. Commun.* **2016**, *7*, 12230.
(32) Syed, I.; de Celis, M. F. R.; Mohan, J. F.; Moraes-Vieira, P. M.; Vijayakumar, A.; Nelson, A. T.; Siegel, D.; Saghatelian, A.; Mathis, D.; Kahn, B. B. PAHSAs attenuate immune responses and promote β cell survival in autoimmune diabetic mice. *J. Clin. Invest.* **2019**, *129*, 3717−3731.
(33) Plötz, T.; von Hanstein, A. S.; Krümmel, B.; Laporte, A.; Mehmeti, I.; Lenzen, S. Structure-toxicity relationships of saturated and unsaturated free fatty acids for elucidating the lipotoxic effects in human EndoC-βH1 beta-cell. *Biochim. Biophys. Acta, Mol. Basis Dis.* **2019**, *1865*, 165525.
(34) Pingitore, A.; Gonzalez-Abuin, N.; Ruz-Maldonado, I.; Huang, G. C.; Frost, G.; Persaud, S. J. Short chain fatty acids stimulate insulin secretion and reduce apoptosis in mouse and human islets in vitro: Role of free fatty acid receptor 2. *Diabetes, Obes. Metab.* **2019**, *21*, 330−339.
(35) Natalicchio, A.; Marrano, N.; Biondi, G.; Spagnuolo, R.; Labarbuta, R.; Porreca, I.; Cignarelli, A.; Bugliani, M.; Marchetti, P.; Perrini, S.; Laviola, L.; Giorgino, F. The myokine irisin is released in response to saturated fatty acids and promotes pancreatic β-cell survival and insulin secretion. *Diabetes* **2017**, *66*, 2849−2856.
(36) Dhayal, S.; Zummo, F. P.; Anderson, M. W.; Thomas, P.; Welters, H. J.; Arden, C.; Morgan, N. G. Differential effects of saturated and unsaturated fatty acids on autophagy in pancreatic β-cells. *J. Mol. Endocrinol.* **2019**, *63*, 285−296.
(37) Eitel, K.; Staiger, H.; Brendel, M. D.; Brandhorst, D.; Bretzel, R. G.; Häring, H.-U.; Kellerer, M. Different role of saturated and unsaturated fatty acids in beta-cell apoptosis. *Biochem. Biophys. Res. Commun.* **2002**, *299*, 853−856.
(38) Němcová-Fürstová, V.; Balušíková, K.; Halada, P.; Pavlíková, N.; Šrámek, J.; Kovář, J. Stearate-induced apoptosis in human pancreatic β-cells is associated with changes in membrane protein expression and these changes are inhibited by oleate. *Proteonomics Clin. Appl.* **2019**, *13*, 1800104.
(39) Yu, H.; Lee, H.; Herrmann, A.; Buettner, R.; Jove, R. Revisiting STAT3 signaling in cancer: New and unexpected biological functions. *Nat. Rev. Cancer* **2014**, *14*, 736−746.
(40) Aaronson, D. S.; Horvath, C. M. A road map for those who don't know JAK−STAT. *Science* **2002**, *296*, 1653−1655.
(41) Niu, J.; Sun, Y.; Chen, B.; Zheng, B.; Jarugumilli, G. K.; Walker, S. R.; Hata, A. N.; Mino-Kenudson, M.; Frank, D. A.; Wu, X. Fatty acids and cancer-amplified ZDHHC19 promote STAT3 activation through S-palmitoylation. *Nature* **2019**, *573*, 139−143.
(42) Furtek, S. L.; Backos, D. S.; Matheson, C. J.; Reigan, P. Strategies and approaches of targeting STAT3 for cancer treatment. *ACS Chem. Biol.* **2016**, *11*, 308−318.

https://dx.doi.org/10.1021/acs.jmedchem.0c00844
J. Med. Chem. XXXX, XXX, XXX−XXX

(43) Wong, A. L. A.; Hirpara, J. L.; Pervaiz, S.; Eu, J.-Q.; Sethi, G.; Goh, B.-C. Do STAT3 inhibitors have potential in the future for cancer therapy? *Expert Opin. Invest. Drugs* **2017**, *26*, 883−887.
(44) Qin, J.; Shen, X.; Zhang, J.; Jia, D. Allosteric inhibitors of the STAT3 signaling pathway. *Eur. J. Med. Chem.* **2020**, *190*, 112122.
(45) Vetere, A.; Choudhary, A.; Burns, S. M.; Wagner, B. K. Targeting the pancreatic β-cell to treat diabetes. *Nat. Rev. Drug Discovery* **2014**, *13*, 278−289.
(46) Bone, R. N.; Gai, Y.; Magrioti, V.; Kokotou, M. G.; Ali, T.; Lei, X.; Tse, H. M.; Kokotos, G.; Ramanadham, S. Inhibition of Ca^{2+}-independent phospholipase $A_2\beta$ (iPLA$_2\beta$) ameliorates islet infiltration and incidence of diabetes in NOD mice. *Diabetes* **2015**, *64*, 541−554.
(47) Dedaki, C.; Kokotou, M. G.; Mouchlis, V. D.; Limnios, D.; Lei, X.; Mu, C. T.; Ramanadham, S.; Magrioti, V.; Dennis, E. A.; Kokotos, G. β-Lactones: A novel class of Ca^{2+}-independent phospholipase A_2 (Group VIA iPLA$_2$) inhibitors with the ability to inhibit β-Cell apoptosis. *J. Med. Chem.* **2019**, *62*, 2916−2927.
(48) Ertunc, M. E.; Kok, B. P.; Parsons, W. H.; Wang, J. G.; Tan, D.; Donaldson, C. J.; Pinto, A. F. M.; Vaughan, J. M.; Ngo, N.; Lum, K. M.; Henry, C. L.; Coppola, A. R.; Niphakis, M. J.; Cravatt, B. F.; Saez, E.; Saghatelian, A. AIG1 and ADTRP are endogenous hydrolases of fatty acid esters of hydroxy fatty acids (FAHFAs) in mice. *J. Biol. Chem.* **2020**, *295*, 5891.
(49) Gómez-Cortés, P.; Juárez, M.; de la Fuente, M. A. Milk fatty acids and potential health benefits: An updated vision. *Trends Food Sci. Technol.* **2018**, *81*, 1−9.
(50) Davoodi, H.; Esmaeili, S.; Mortazavian, A. M. Effects of milk and milk products consumption on cancer: A review. *Compr. Rev. Food Sci. Food Saf.* **2013**, *12*, 249−264.
(51) Aune, D.; Lau, R.; Chan, D. S. M.; Vieira, R.; Greenwood, D. C.; Kampman, E.; Norat, T. Dairy products and colorectal cancer risk: A systematic review and meta-analysis of cohort studies. *Ann. Oncol.* **2012**, *23*, 37−45.
(52) Murphy, N.; Norat, T.; Ferrari, P.; Jenab, M.; Bueno-de-Mesquita, B.; Skeie, G.; Olsen, A.; Tjønneland, A.; Dahm, C. C.; Overvad, K.; Boutron-Ruault, M. C.; Clavel-Chapelon, F.; Nailler, L.; Kaaks, R.; Teucher, B.; Boeing, H.; Bergmann, M. M.; Trichopoulou, A.; Lagiou, P.; Trichopoulos, D.; Palli, D.; Pala, V.; Tumino, R.; Vineis, P.; Panico, S.; Peeters, P. H. M.; Dik, V. K.; Weiderpass, E.; Lund, E.; Garcia, J. R. Q.; Zamora-Ros, R.; Pérez, M. J. S.; Dorronsoro, M.; Navarro, C.; Ardanaz, E.; Manjer, J.; Almquist, M.; Johansson, I.; Palmqvist, R.; Khaw, K.-T.; Wareham, N.; Key, T. J.; Crowe, F. L.; Fedirko, V.; Gunter, M. J.; Riboli, E. Consumption of dairy products and colorectal cancer in the European prospective investigation into cancer and nutrition (EPIC). *PloS One* **2013**, *8*, No. e72715.
(53) Kuntz, S.; Wenzel, U.; Daniel, H. Comparative analysis of the effects of flavonoids on proliferation, cytotoxicity, and apoptosis in human colon cancer cell lines. *Eur. J. Nutr.* **1999**, *38*, 133−142.
(54) Geng, T.; Hu, W.; Broadwater, M. H.; Snider, J. M.; Bielawski, J.; Russo, S. B.; Schwacke, J. H.; Ross, J.; Cowart, L. A. Fatty acids differentially regulate insulin resistance through endoplasm reticulum stress-mediated induction of tribbles homologue 3: A potential link between dietary fat composition and the pathophysiological outcomes of obesity. *Diabetologia* **2013**, *56*, 2078−2087.
(55) Imamura, F.; Fretts, A.; Marklund, M.; Korat, A. V. A.; Yang, W.-S.; Lankinen, M.; Qureshi, W.; Helmer, C.; Chen, T. A.; Wongm, K. L.; Bassett, J. K.; Murphy, R.; Tintle, N.; Yu, C. I.; Brouwer, I. A.; Chien, K. L.; Frazier-Wood, A.; Del Gobbo, L. C.; Djoussé, L.; Geleijnse, J. M.; Giles, G. G.; de Goede, J.; Gudnason, V.; Harris, W. S.; Hodge, A.; Hu, F.; Koulman, A.; Laakso, M.; Lind, L.; Lin, H. J.; McKnight, B.; Rajaobelina, K.; Risérus, U.; Robinson, J. G.; Samieri, C.; Siscovick, D. S.; Soedamah-Muthu, S. S.; Sotoodehnia, N.; Sun, Q.; Tsai, M. Y.; Uusitupa, M.; Wagenknecht, L. E.; Wareham, N. J.; Wu, J. H.; Micha, R.; Forouhi, N. G.; Lemaitre, R. N.; Mozaffarian, D. Fatty acid biomarkers of dairy fat consumption and incidence of type 2 diabetes: A pooled analysis of prospective cohort studies. *PLoS Med.* **2018**, *15*, No. e1002670.
(56) Liu, S.; van der Schouw, Y. T.; Soedamah-Muthu, S. S.; Spijkerman, A. M. W.; Sluijs, I. Intake of dietary saturated fatty acids and risk of type 2 diabetes in the European Prospective Investigation into Cancer and Nutrition-Netherlands cohort: associations by types, sources of fatty acids and substitution by macronutrients. *Eur. J. Nutr.* **2019**, *58*, 1125−1136.
(57) Bourboula, A.; Limnios, D.; Kokotou, M. G.; Mountanea, O. G.; Kokotos, G. Enantioselective organocatalysis-based synthesis of 3-hydroxy fatty acids and fatty γ-lactones. *Molecules* **2019**, *24*, 2081.
(58) Mohapatra, D. K.; Bhattasali, D.; Gurjar, M. K.; Khan, M. I.; Shashidhara, K. S. First asymmetric total synthesis of penarolide sulfate A1. *Eur. J. Org. Chem.* **2008**, 6213−6224.
(59) Chow, S.; Kitching, W. Hydrolytic kinetic resolution of terminal mono- and bis-epoxides in the synthesis of insect pheromones: routes to (−)-(R)- and (+)-(S)-10-methyldodecyl acetate, (−)-(R)-10-methyl-2-tridecanone, (−)-(R)-(Z)-undec-6-en-2-ol (Nostrenol), (−)-(1R,7R)-1,7-dimethylnonyl propanoate, (−)-(6R,12R)-6,12-dimethylpentadecan-2-one, (−)-(2S,11S)-2,11-diacetoxytridecane and (+)-(2S,12S)-2,12-diacetoxytridecane. *Tetrahedron: Asymmetry* **2002**, *13*, 779−793.

https://dx.doi.org/10.1021/acs.jmedchem.0c00844
J. Med. Chem. XXXX, XXX, XXX−XXX